بسم الله الرحمن الرحيم

ACCIDENT INVESTIGATION COORDINATING COMMITTEE

SERIOUS INCIDENT INVESTIGATION REPORT 2024/02

FINAL REPORT
ON INVESTIGATION OF THE SERIOUS INCIDENT INVOLVING
DHC-6-300, 8Q-TMO AIRCRAFT
AT WESTIN MALDIVES (MIRIANDHOO) WATER AERODROME,
ON 09 JUNE 2024

INTRODUCTION

Maldives is a signatory to the Convention on International Civil Aviation (Chicago, 1944) which established the principles and arrangements for the safe and orderly development of international air transport. Article 26 of the Convention obligates Signatories to investigate accidents and serious incidents to civil aircraft occurring in their State.

This report is based upon the investigation carried out by the Accident Investigation Coordinating Committee (AICC) in accordance with Annex 13 to the Convention, the Civil Aviation Act 2/2001 and the Civil Aviation Regulations. The sole objective of this investigation is to prevent accidents and serious incidents. It is not the purpose of this investigation to apportion blame or liability as envisaged in Annex 13 to the Convention.

In investigating this serious incident, AICC was assisted by Maldives Civil Aviation Authority (MCAA), and Trans Maldivian Airways.

All timings in this report are in local time unless otherwise stated. Time difference between local and UTC is +5 hrs.

The report is released 14 September 2025.

Mr. Abdul Razzak Idris
Chairperson
Accident Investigation Coordinating Committee

TABLE OF CONTENTS

LIST OF ABBREVIATIONS

AICC : Accident Investigation Coordinating Committee
ATL : Aircraft Technical Log
CVR : Cockpit Voice Recorder
DHC-6-300 : Viking Air Twin Otter 300 series aircraft
EDS : Energy Dispersive X-ray Spectroscopy
ELT : Emergency Locator Transmitter
EMMA : Equalized Maintenance for Maximum Availability
FDR : Flight Data Recorder
FIN : Operator designated 3 letter code for Miriandhoo water aerodrome
FO : First Officer
FWD : Forward
lbs. : Pounds
ICA : Instructions for Continued Airworthiness
IGSCC : Intergranular Stress Corrosion Cracking
LH : Left Hand
LOPA : Layout of Passenger Accommodation
MCAA : Maldives Civil Aviation Authority
MCAR : Maldives Civil Aviation Regulations
MLE : IATA designated three letter code for Velana International Airport
MTOM : Maximum Take-Off Mass
PIC : Pilot-in-command
RH : Right Hand
STC : Supplemental Type Certificate
SEM : Scanning Electron Microscopy
TAC : Total Air Cycles
TAT : Total Air Time
TBD : To be determined
T/O : Take-Off
TMA : Trans Maldivian Airways Pvt. Ltd.
UTC : Coordinated Universal Time
VIA : Velana International Airport
WST : Operator designated 3 letter code for Westin Maldives water aerodrome

SYNOPSIS

On Sunday 9 June 2024, at about 1515 hours local time, Twin Otter (DHC-6-300 series, MSN 234) floatplane, registration 8Q-TMO, landed at Miriandhoo Westin Maldives water aerodrome. Upon applying reverse thrust, an unusual sound was heard, and the aircraft banked to the right. The PIC shut down both engines and brought aircraft to rest. The crew observed that the right float was detached.

All the passengers were safely disembarked onto dinghies and taken to the resort. The aircraft was towed with the assistance of speed launches and dinghies and beached on the island. By the time the aircraft was beached, it had partially submerged in water. The crew disembarked through the main door after the aircraft had been beached and secured.

1.0 FACTUAL INFORMATION

Legal Owner:	Trans Maldivian Airways Pvt Ltd.
Registered owner:	Trans Maldivian Airways Pvt Ltd.
Operator:	Trans Maldivian Airways Pvt Ltd.
	(Air Operator Certificate No.005)
Aircraft Type:	De Havilland Aircraft of Canada Ltd. DHC-6-300
Nationality:	Republic of Maldives
Registration:	8Q-TMO
Aircraft Manufacturer:	The de Havilland Aircraft Company of Canada, Limited
Manufacturers Serial No.:	234
Place of Accident:	The Westin Maldives Miriandhoo (Baa Atoll)
Latitude:	N 05° 03’ 53.00”,
Longitude:	E 73° 01’ 45.10”
Date and Time:	09 June 2024; 1515 hours

1.1 History of Flight

1.1.1 Background

Aircraft bearing registration 8Q-TMO was released from the operator’s main base, after the Daily Inspection at 0816 hours, at the main base (MLE), on a multisectoral flight FLT994896 with routing MLE-FIN-WST-MLE. The aircraft departed MLE (dock off) on MLE-FIN sector at 1121 hours on 09 June 2024, as per ATL page (Log No 188510) opened for the day by the Operator. It took off from MLE at 1131 hours and landed at FIN at 1205 hours, without incident. For the second sector (FIN-WST), the aircraft took off from FIN at 1508 hours with 07 passengers and 03 crew and landed at WST at 1511 hours.

Take off Mass of the aircraft when it departed FIN was 11,067 lbs., which notably is far below the maximum take off mass of 12,500 lbs. The aircraft had 750 lbs. of fuel onboard confirmed from the ATL page.

The condition of the sea at the aerodrome when the aircraft landed was calm, despite the aerodrome being classified as a "C" Category aerodrome where only the PIC is authorized to land (restriction imposed by the Operator).

Soon after landing, the pilots heard a thud from outside, indicating that something abnormal had occurred, followed by the aircraft tilting towards the right hand. When the FO was asked by the PIC to check outside for any abnormalities, FO said that the float on his side was not upright, and the wing was drooping. Knowing the problems normally associated with detachment of the float, PIC as the Pilot Flying, as precautionary action, decided to shut both engines down to prevent the right-hand propeller striking the float causing further damage to both propeller and float.

Rescue efforts were initiated immediately: PIC instructed cabin crew and passengers to remove the life jackets from their stowage. In minutes, launches and dinghies rushed to the incident scene. All passengers disembarked on to the boats safely and were taken to Westin Maldives resort.

With both PIC and FO still onboard, the aircraft was towed to the beach and secured for investigation.

1.2 Injury to Persons

Injuries	Flight Crew	Cabin Crew	Passengers	Others
Fatal	0	0	0	Nil
Serious	0	0	0	Nil
Minor	0	0	0	Nil
Nil	2	1	7	Nil
Total	2	1	7	Nil

1.3 Damage to aircraft

The survey carried out collectively by CAA Airworthiness, AICC and TMA Safety post-serious incident revealed:

1. Aft Spreader Bar:
    - RH attachment point completely detached and submerged.
    - Attachment bolt missing; indicating that the bolt sheared.

2. RH propeller impacted float, damaging prop and fuselage, consequential damage.
3. Forward Spreader Bar:
   - Remained attached to the floats.
   - Flywires damaged, jury strut detached from fuselage.
   - RH stairs detached (likely during beaching).
   - LH float strut cover damaged due to float spreading.
   - Wing fairings and sling points inspected; attachment points secure.
   - RH aft attachment broken; forward point cracked.

The extent of the damage sustained by the Floats as well as airframe structures and airframe components can be captured from the photo images shown in the table below.

<table>
<tr>
<td> 
Spreader bar attaching lug - float</td>
<td> 
Aircraft Beached at Westin Resort</td>
<td> 
RH propeller impacted with RH float</td>
</tr>
<tr>
<td> 
FWD spreader bar remains attached.</td>
<td> 
Flywire ruptured</td>
<td> 
Failed lugs on AFT fitting – spreader bar</td>
</tr>
</table>

1.4 Personnel information

1.4.1 Pilot-In-Command

Age:	36
Nationality:	Maldivian
Gender:	Male
Type of License:	CPL-A
License issued on: License expires on:	16 November 2015 15 November 2027
Type of medical:	Class One
Medical issued on:	3 January 2024
Medical expires on:	2 January 2025
Types flown:	DHC-6
Hrs. on type:	7,142
Ratings:	DHC6-Sea
Last Proficiency check:	13 August 2023
Total hrs. as PIC:	4,249
Total flight time:	
Last 90 days:	176.8
Last 28 days:	27.9
Last 24 hrs.:	5.4
Previous rest period:	5 – 7 June 2024

1.4.2 Co-pilot

Age:	30
Nationality:	Maldivian
Gender:	Male
Type of License:	CPL-A
License issued on:	28 November 2022
License expires on:	27 November 2027
Type of medical:	Class One
Medical issued on:	20 November 2023
Medical expires on:	19 November 2024

Types flown:		DHC-6
Hrs. on type:		1,090
Ratings:		DHC-6
Last Proficiency check:		14 May 2024
Total flight time:		
	Last 90 days:	154.6
	Last 28 days:	25.5
	Last 24 hrs.	2.4
Previous rest period:		5 – 7 June 2024

1.4.3 Cabin Crew

Age:	19
Nationality:	Maldivian
Gender:	Male
Type of License:	CCL
License issued on:	14 April 2024
License expires on:	13 April 2029
Type of medical:	Class Three
Medical issued on:	27 February 2024
Medical expires on:	27 February 2026
Previous rest period:	4 – 6 June 2024

1.5 Aircraft information

1.5.1 General information

The DHC-6-300 “Twin Otter” is an unpressurised, all-metal, high wing aircraft powered by two Pratt & Whitney PT6A-27 engines driving three-bladed, reversible-pitch, full feathering propellers manufactured by Hartzell Propeller Inc. The aircraft is designed for seating two pilots, side by side with dual controls and ASPEN Avionics.

Manufacturer:	The de Havilland Aircraft Company of Canada, Limited
Registration:	8Q-TMO

Powerplants:	PT6A-27
Manufacturer's Serial Number (MSN):	234
Year of construction:	1969
Total Air Time and Landings at time of incident:	53,954.67 hrs. and 110,224 landings
Certificate of Airworthiness:	Normal category, issued on 29 January 2009
Airworthiness Review Certificate:	Issued on - 26 January 2024 - extended until 26 January 2025
Last periodic inspection	EMMA No 34 on 09 May 2024
Last inspection carried out TAT / CYC	53,878.21 hrs / 110,038 cycles

Last Daily Inspection was carried out at 0816 hrs on 09 June 2024, and the last engine wash was recorded as carried out on 07 June 2024.

1.5.2 Engines and Propellers

Right Engine (Gas Generator)	
Right engine manufacturer	Pratt & Whitney Canada
Year of manufacture	Uknown
Model	PT6A-27
Serial number	PCE-PG0363
Total Hrs. since new	9,980.16
Last overhaul date	19 Dec 2023
Hrs. since overhaul	596.96
Last check carried out	EMMA # 34 on 09 May 2024
Hrs. since last check	76.46 Hrs.

Left Engine (Gas Generator)	
Left engine manufacturer:	Pratt & Whitney Canada
Year of manufacture:	Uknown
Model:	PT6A-27
Serial number:	PCE-PG0326
Total hrs. since new:	15,142.87

Last overhaul date:	21 April 2021
Hrs. since overhaul:	4,279.67
Last check carried out:	EMMA # 34 on 09 May 2024
Hrs. since last check:	76.46 Hrs.

Right Propeller	
Manufacturer:	Hartzell
Year of manufacture:	Uknown
Model:	HC-B3TN-3DY
Serial number:	BUA31963
Last overhaul date:	29 Jun 2022
Hrs. since last overhaul:	2,229.70 Hrs.
Last check carried out:	EMMA # 34 on 09 May 2024
Left Propeller	
Manufacturer:	Hartzell
Year of manufacture:	Uknown
Model:	HC-B3TN-3DY
Serial number:	BUA21034
Last overhaul date:	04 Oct 2022
Hrs. since last overhaul:	2,274.60 Hrs.
Last check carried out:	EMMA # 34 on 09 May 2024

1.5.3 Cabin Layout and Configuration

Cabin was configured under a LOPA approved by an EASA approved Design Organization to carry fifteen passengers and one cabin crew in a standard floatplane configuration. In this configuration the double-seat in the sixth-row position is removed for carriage of passenger luggage in the cabin rather than carrying them in the dedicated cargo compartments. The reason being that the forward cargo compartment is not accessible for loading the luggage while the aft cargo compartment is not large enough to accommodate all the luggage normally carried by fifteen passengers. The aft baggage compartment is only used for loading smaller luggage.

The aircraft was in float configuration with Wipline 13000 floats (manufactured by Wipaire) installed. The aircraft had six emergency exits, of which, the right aft cabin door is approved to be blocked.

1.5.4 Flight Controls

The flight controls consist of conventional, manually actuated primary flight controls operated through cables, pulleys, and mechanical linkages. Rudder and elevator trim are manually controlled and mechanically actuated; aileron trim is electrically actuated. Secondary flight controls consist of hydraulically actuated wing flaps.
No abnormalities were reported on any of the flight controls or related systems.

1.5.5 Fuel

Jet A-1 fuel was used on aircraft engines.

1.5.6 Accessories

Not applicable.

1.5.7 Recent maintenance:

The most recent maintenance inspections carried out include Equalized Maintenance for Maximum Availability (EMMA) check number 34 complied with on 09 May 2024, at 53,878.21 TAT and 110,038 TAC.

Float 600 hours (DeHavilland) check complied with on 23 April 2024 at 53,818.24 hours (TAT), 109,889 cycles (TAC). The last of the three checks calls for inspection of the float landing gear attachment fittings including lugs and brackets for condition, cracks, corrosion and security. The inspection requires removal of float attachment bolts, one at a time to inspect for wear, scoring and ovality.

Corrective Action field of the Task Card completed reads: "*Float landing gear attachments and hardware inspection carried out i.a.w. Wipaire Service Manual REV N. Found LH aft steps lower FWD slide fitting (male) worn. LH V strut top attachment bolt with pitting and RH pylon top attachment bolt worn. RH top attachment bolt replaced, LH aft steps lower FWD slide fitting (male) replaced and LH V strut top attachment bolt, bushings*

replaced i.a.w. Wipaire Service Manual REV N. Found SAT. Bushing – P/N: 13A02512-003, B/N: 387820 & P/N: PDMC6FSM1522-31, B/N: 391968, slide fitting – P/N: 8A02273-007, B/N: 398960".

From the above, it is apparent that no parts (fitting, bolts, bushings) were replaced on the right side of the aft spreader bar fittings during the last float inspections (50, 100, 600 hourly inspections carried out prior to the serious incident occurred.

1.5.8 Defects

The aircraft had no open deferred defects recorded on the day of the serious incident.

1.5.9 Aircraft load

- CG values during operations remained within limits:
- MLE to FIN: 12,500 lbs., CG 32% MAC
- FIN to WST: 11,662.70 lbs., CG 29% MAC (Range: 25%–32%)

An electronic Mass and Balance Report generated by the Flight crew before departure was available on the tablet. According to this report, the CG for take-off from Miriandhoo water aerodrome and estimated landing at destination remains within prescribed limitations.

1.6 Meteorological information

No recorded weather data was available at Miriandhoo – Westin Maldives water aerodrome. The nearest weather data was available at Dharavandhoo automatic weather station, which is approximately 15 km to Miriandhoo water aerodrome. At 15:00 hrs on 09 June 2024 the mean value of the wind speed varied between 18-21 knots and that of the gust speed varied from 19 to 21 knots from WSW direction. No rainfall was reported either.

1.7 Aids to navigation

The aircraft was operating under VFR, where no navigational aids were required.

1.8 Communications

There were no communication problems or system anomalies throughout the flight.

1.9 Aerodrome information

Miriandhoo - Westin Maldives Aerodrome
GPS Reference - N 05° 03’ 47.00”, E 73° 01’ 52.20”
Aerodrome license number AP/0/153 was issued to Trans Maldivian Airways Pvt. Ltd., on 18 February 2021.

1.10 Flight Recorders

No flight data recorder (FDR) or cockpit voice recorder (CVR) was installed on the aircraft, as MCARs do permit operation of the DHC-6 aircraft Series 100/200/300 aircraft without them.

1.11 Wreckage and impact information

Not applicable.

1.11.1 Incident site visit

The incident site was visited by investigators from both MCAA and AICC. During this visit the aircraft was visually checked for damage. The aircraft system functional checks were carried out as far as possible except for the RH engine run.

1.11.2 Wreckage Condition

Refer to paragraph 1.3 for damages information.

1.11.3 Salvage operations

A speed boat and two dinghies were used for the rescue and passenger evacuation. The aircraft was first towed to the shallower waters using a speedboat and then pulled up to the beach using ropes and winch cables.

1.12 Medical and pathological information

Both flight crew members and the cabin crew were subjected to drug tests and the results were reported negative for all three crew members.

1.13 Fire

There were no fire or fire alarms.

1.14 Survival Aspect

Shortly after detachment of the right-hand float from the fuselage, passengers were rescued using speed launches and dinghies. The aircraft was towed with the assistance of the dinghies and beached on the island. By the time the aircraft was beached, the aircraft was partly submerged.

1.15 Tests and research

Failed fittings (rear spreader bar, right hand side) were shipped to Wipaire (Float Manufacturer) for metallurgical evaluation along with a few of the bolts used to secure the spreader bar to the floats. A total of six samples were shipped to Wipaire. These were in turn sent to Element Materials Technology based in the USA where all samples were evaluated and reports generated. The reports referenced ENB037175P (Element Report# 1) and ENB037181P (Element Report# 2) are inserted into this Investigation Report under section Appendices.

1.16 Organizational and Management Information

TMA is an MCAA approved Air Operator Certificate (AOC-005) holder, with Continuing Airworthiness Management Organization (CAMO) Approval MV.CAMO.003. TMA provides domestic air services with a fleet of 65 DHC-6 aircraft on floats. The company is authorized to conduct day VFR Operations. The company holds Approved Maintenance Organization Approval reference MV.145.025 issued by the MCAA.

1.17 Additional Information

None

2.0 ANALYSIS

The analysis considers operational aspects, environmental conditions, aircraft and its systems performance, maintenance history, Instruction for Continued Airworthiness (ICA) and human factors leading to the serious incident. Particular attention is given to the impact of saltwater exposure on the structural components, float integrity: float attachment fittings and bolts.

Although the aerodrome is classified as a Category “C” where landing is restricted by the operator for PICs, the prevailing condition at the time of landing was relatively calm. According to the PIC he was able to land the aircraft normally without much

ado. The pilots held valid licenses and medical reports and maintained validity of their proficiency checks, thus, there is no reason to believe that operational aspects contributed to the serious incident.

The aircraft was installed with floats under Wipaire Supplemental Type Certificate (STC), validated by CAA Maldives under their reference MOD-DHC6-2010-06R1 - Wipline 13000. Failure of the rear spreader bar fittings and bolts prompted AICC to focus more on the metallurgical analysis carried out by Wipaire – manufacturer of the parts.

The serious incident prompts comparing ICAs provided by the STC and TC holders for floatplane and landplane versions of the same aircraft model. The inspections and their intervals on ATA Chapter 32 are tabulated below.

		Inspection/Overhaul Requirements	
Interval	**Float LDG (STC)**	**Float LDG (TC/PSM 1-6-7)**	**Wheel LDG (TC/PSM 1-6-7)**
50	x	x	
100	x	x	
200	x	x	x
300		x	
600		x	
7000 LD, 5 YR			x

X denotes – applicable

Following review of the scheduled intervals and inspection requirements, it is apparent that the wheel landing gears installed on land-operated aircraft require periodic overhauls while the float landing gears, serving the same purpose on floatplanes, do not require, although the water aerodromes used for landing/taking off floatplanes are subjected to more hostile environments (rough and saline water conditions) whilst operated in the Maldives. The ICAs of both TC and STC holders for wheel and float landing gear, arguably require review of ATA chapter 32. While the Supplements approved for STCs in general make references to TC holders ICAs, no

such references are made to the TC holders (PSM) Manuals in the case of the Wipaire float STC.

Maintenance records indicate that all scheduled inspections were carried out in accordance with the operator's maintenance program. Prior to failure of the fitting, a scheduled 600 hourly inspection was carried out at a time for wear, scoring and ovality) at 53,818.24 hours and 109,889 cycles on 23 April 2024 (TMA Task Card # 240271-296). In this inspection, float landing gear attachment fittings including lugs and brackets were inspected for condition, cracks, corrosion and security including float attachment bolts (after removing them). However, the corrosion that led to the failure of the fitting went unnoticed. Notably, this failure occurred after 136.43 hours and 335 cycles since last 600 hourly inspection carried out.

The operator's corrosion control program, though compliant with STC holders ICA, may not have adequately addressed the real-world severity of the operating environment prevailing in the Maldives. Furthermore, the material composition of the rear spreader bar fitting—typically an aluminum alloy—makes it susceptible to both galvanic corrosions, especially if in contact with dissimilar metals, particularly where drainage or protective coating effectiveness is compromised.

The failure of the rear spreader bar fitting on the right float occurred during normal operations under relatively benign weather conditions, with no known excessive loads or abnormal maneuvers. The environmental context—a harsh, salt-laden operating area—necessitates enhanced vigilance in the detection and mitigation of corrosion and structural degradation, especially on components such as spreader bars and float attachment fittings that are repeatedly exposed to saltwater spray, immersion, and varying load cycles.

There is no evidence of pilot error, loading irregularities, or weather-related stresses contributing to the failure. This strongly indicates that the failure was progressive in nature, rooted in a combination of environmental exposure, possible design or material vulnerabilities, and limitations in inspection detectability under current maintenance protocols.

Metallurgical Evaluation of Floatplane Fittings and Bolts

Failure of the right-hand rear spreader bar fitting prompted AICC/CAA Maldives to carry out metallurgical evaluations collaboratively on the failed fitting as well as bolts and fittings from the other (left hand) side and the front spreader bar right hand fitting. Two separate reports were generated; Report #1 referenced ENB037175P covered the serviceable fittings (three each) and bolt (three each), while Report #2, referenced ENB037181P, evaluated the fractured in-service fitting. Both evaluations were carried out at Element Materials Technology, USA, at the request AICC, with Wipaire being the coordinator.

Tests conducted include, but are not limited to:

1. Visual Examination
2. SEM (Scanning Electron Microscopy)
3. Chemical Analysis (OES)
4. Metallography
5. Microhardness Testing (Knoop, HK 0.5)

Report 1: Condition Assessment of Bolts and Fittings (ENB037175P)

Three bolts and three corresponding fittings (referred to as rear spreader bar LH, front spreader bar LH and front spreader bar RH) were examined for signs of material degradation or failure, particularly fatigue. Each bolt and fitting were inspected visually, chemically analyzed, scanned under SEM, subjected to metallography, and tested for microhardness.

From the results of the evaluations carried out there is no evidence of fatigue cracking or catastrophic failure observed in any component. However, the metallographic evaluation of Bolt 1 (Fig. 10) showed that it was exhibiting branching cracks at thread tips. All bolts were confirmed to be Grade 8640 steel with a tempered martensite microstructure, and fittings were of 2024 aluminum alloy. Surface inclusions (Fig. 12 and 16) were observed at or near the surface of the bolt holes of all fittings, which may serve as stress concentration sites.

Report 2: Failure Analysis of Fractured Fitting (ENB037181P)

The report states that the cracked fitting (P/N 13A03030-004) showed significant corrosion damage. The hours and cycles accrued on the part could not be

determined, the reason being that it is not a serialized component and hence classified as a consumable.

Evaluation of the fitting concluded that the failure was attributed to intergranular stress corrosion cracking (IGSCC), initiated at a pitting corrosion site that developed at the bore of the lug (Fig. 8). Cracking propagated along elongated grain boundaries, consistent with IGSCC caused by applied stress and a corrosive environment, which is the case in the Maldives, given the chloride-rich environment. SEM/EDS analysis reaffirms this, showed high chlorine content in corrosion products, indicating a marine-induced corrosion mechanism. Protective coatings were missing at the crack origin, likely worn off during service. No evidence of overload or fatigue fracture was found, confirming environmental-stress synergy as the root cause.

3.0 CONCLUSIONS:

3.1 Causes

The cause of this serious incident was due to the failure of the right-hand aft spreader bar float attachment lug and the bolt during the landing phase. The bolt was missing and could not be found. This failure occurred due following reason;

1. Intergranular Stress Corrosion Cracking (IGSCC): The primary cause of failure was identified as IGSCC, which initiated from pitting corrosion at the bore of the fitting lug, exacerbated by exposure to seawater (Figures 1-13).

2. Corrosive environment: The fitting was exposed to seawater, and inadequate lubrication and potential galvanic corrosion (if dissimilar materials were used) contributed to the cracking (Figures 4-13).

3.2 Contributing factors

The AICC determines that the contributing factors of this serious incident are as specified below:

1. Surface degradation: The fitting's surface showed signs of wear, including the loss of paint and epoxy coating, which would have protected it from corrosive elements (Figures 2-5).

2. Corrosion-induced cracking: The pitting corrosion likely formed between the bore and the bolt due to crevice corrosion, which was further aggravated by the lack of surface coatings (Figures 5-13).

3. Presence of intermetallic particles: Corrosion preferentially attacked areas containing intermetallic particles, particularly copper-rich phases, making these areas more susceptible to stress corrosion (Figures 14-17).

4.0 SAFETY RECOMMENDATIONS

4.1 Recommendation to Operator

Based on the metallurgical findings, the investigation highlights the need for taking preventative measures primarily to avoid similar failures in the future:

1. Implement scheduled detailed inspections of all float fitting lugs and bolts for signs of corrosion, paint/coating damage, or cracking. Given that IGSCC can progress internally, use non-destructive inspection techniques (dye penetrant or eddy current testing) focused on the lug bore areas to detect any cracks that may initiate at bolt holes in close coordination with STC holder.

2. Ensure that the protective finishes on the fittings (primer and paint) are intact and renewed as necessary. Any paint/primer wear in areas like the bolt bore or lug surface should be promptly touched up to restore a barrier against moisture ingress.

4.2 Recommendation to Float STC holder Wipaire

1. Evaluate manufacturing and supplying spreader bar fittings with more corrosion-resistant alloys, to minimize crevice geometry and enhance paint adhesion to ensure fittings and bolts manufactured for installation are matched in electrochemical potential, where possible. The fittings supplied by the STC holder as replacement fittings are serialized and meet Part 21 requirements for traceability and tractability by the operator(s).

2. Review ICA to add a discard life for all spreader bar fittings and bolts installed on aircraft operated in harsh, saline environments such as those prevailing in the Maldives.

3. Review ICA inspection requirements to be aligned with that of the TC holder (DeHavilland Aircraft of Canada).

4.3 Recommendation to the MCAA

1. Establish procedures to ensure that the recommendations set forth for both the Operator and STC holder are implemented to prevent recurrence of such serious incidents in the future.

5.0 APPENDICES

5.1 ATL page – 188510 dated 09 June 2024

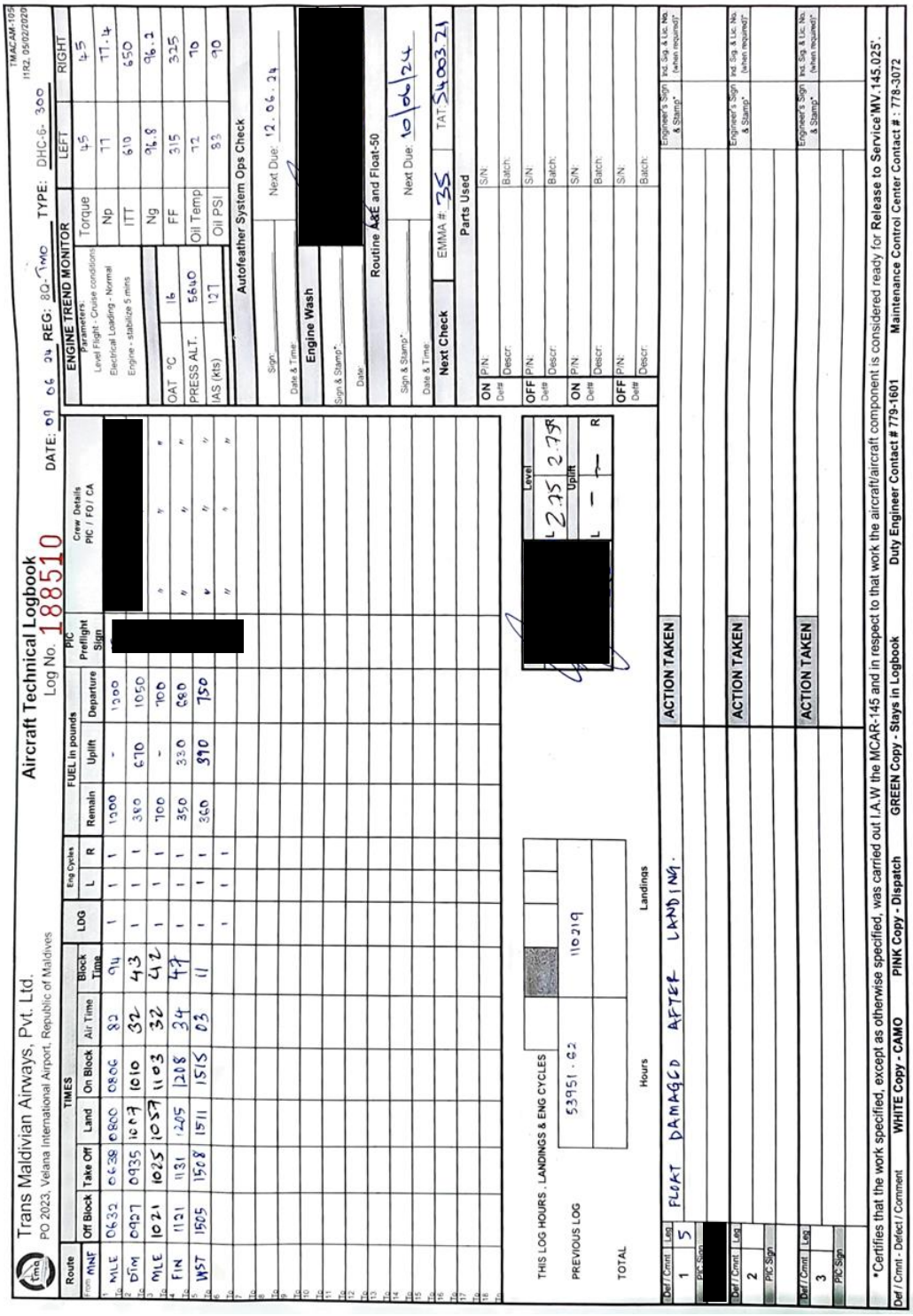

Aircraft Technical Logbook
Log No. 188510

Trans Maldivian Airways, Pvt. Ltd.
PO 2023, Velana International Airport, Republic of Maldives

DATE: 09 06 24 REG: 8Q-TMO TYPE: DHC-6-300

TMACAM-105
Iss. 05/02/2020

Route	TIMES					LDG	Eng Cycles		FUEL in pounds			PIC Preflight Sign	Crew Details PIC / FO / CA
From MNF	Off Block	Take Off	Land	On Block	Air Time	Block Time	L	R	Remain	Uplift	Departure		
1 MLE	0632	0638	0800	0806	82	94	1	1	1900	-	1900		
2 DIM	0927	0935	1047	1050	43	43	1	1	380	670	1050		
3 MLE	1021	1025	1037	1103	32	42	1	1	700	-	700		
4 FIN	1121	1131	1205	1208	34	47	1	1	350	330	680		
5 MST	1505	1508	1511	1515	03	11	1	1	360	390	750		
6							1	1					
7													
8													
9													
10													
11													
12													
13													
14													
15													
16													
17													
18													

" " " "

ENGINE TREND MONITOR Parameters

	Torque	LEFT	RIGHT
Level Flight - Cruise conditions			
Electrical Loading - Normal	Np	77	77.4
Engine - stabilize 5 mins	ITT	610	650
	Ng	96.8	96.2
OAT °C 16	FF	315	325
PRESS ALT. 5640	Oil Temp	72	70
IAS (kts) 127	Oil PSI	93	90

Autofeather System Ops Check
Sign: Next Due: 12.06.24
Date & Time:

Engine Wash
Sign & Stamp*:
Date:

Routine A&E and Float-50
Sign & Stamp*: Next Due: 10/06/24
Date & Time:

Next Check EMMA # 35 TAT 34003.21

Parts Used

ON	P/N:	S/N:	
Def#	Descr:	Batch:	
OFF	P/N:	S/N:	
Def#	Descr:	Batch:	
ON	P/N:	S/N:	
Def#	Descr:	Batch:	
OFF	P/N:	S/N:	
Def#	Descr:	Batch:	

THIS LOG HOURS, LANDINGS & ENG CYCLES
PREVIOUS LOG 53951.92 110219
TOTAL
Hours Landings

Level L 2.5 2.75
Uplift L — — R

Def / Cmnt	Leg	ACTION TAKEN	Engineer's Sign & Stamp*	Ind. Sig & Lic. No (when required)*
1	5	FLOAT DAMAGED AFTER LANDING.		
PIC Sign				
Def / Cmnt	Leg	ACTION TAKEN	Engineer's Sign & Stamp*	Ind. Sig & Lic. No (when required)*
2				
PIC Sign				
Def / Cmnt	Leg	ACTION TAKEN	Engineer's Sign & Stamp*	Ind. Sig & Lic. No (when required)*
3				
PIC Sign				

*Certifies that the work specified, except as otherwise specified, was carried out I.A.W the MCAR-145 and in respect to that work the aircraft/aircraft component is considered ready for Release to Service'MV.145.025'.

Def / Cmnt - Defect / Comment WHITE Copy - CAMO PINK Copy - Dispatch GREEN Copy - Stays in Logbook Duty Engineer Contact # 779-1601 Maintenance Control Center Contact # : 778-3072

5.2 Operational Flight Plan – Day/VFR – Flight Release

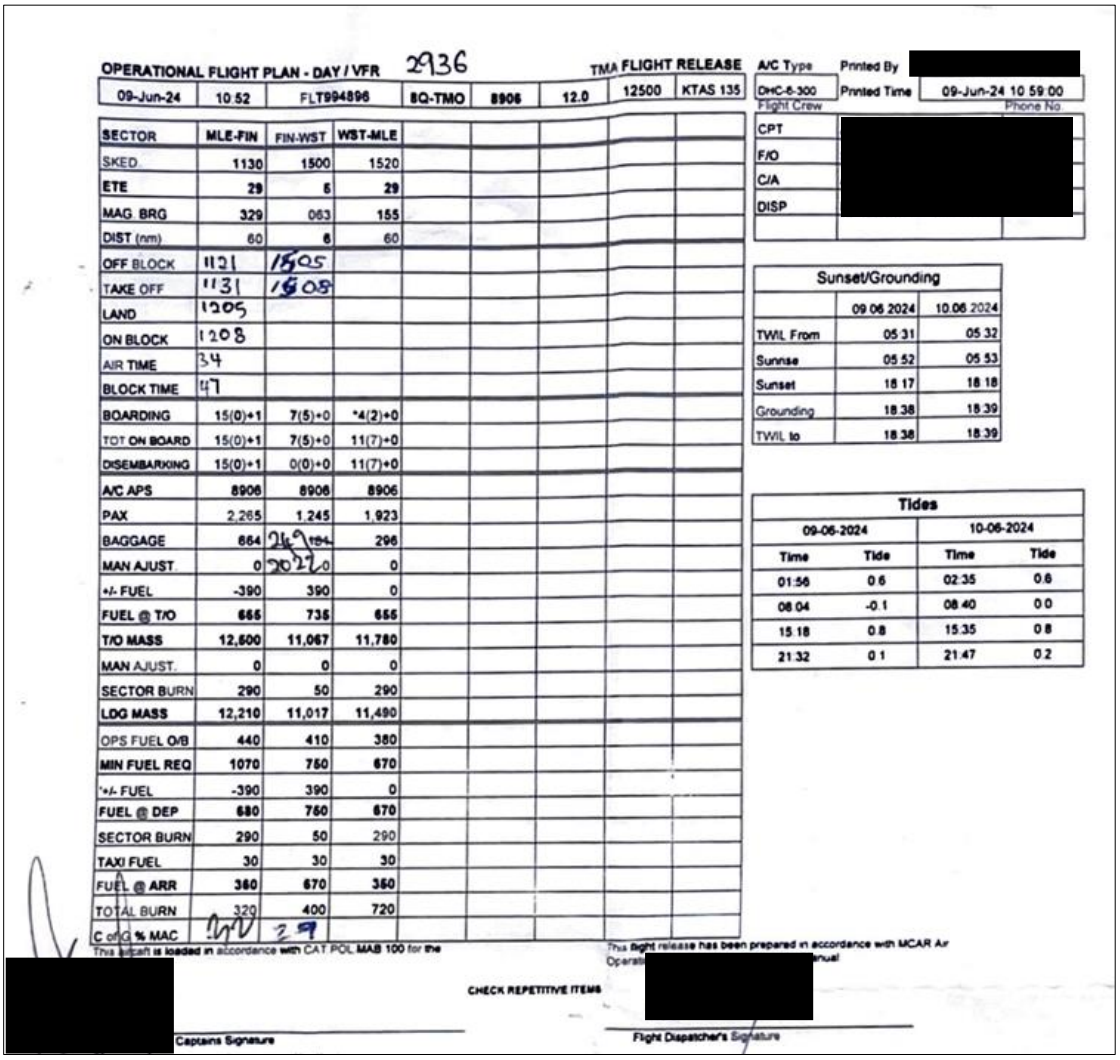

OPERATIONAL FLIGHT PLAN - DAY / VFR 2936 TMA FLIGHT RELEASE

09-Jun-24	10.52	FLT994896	8Q-TMO	8906	12.0	12500	KTAS 135

A/C Type: DHC-6-300 Printed By: [redacted] Printed Time: 09-Jun-24 10 59 00

Flight Crew — Phone No

CPT [redacted]
F/O
C/A
DISP

SECTOR	MLE-FIN	FIN-WST	WST-MLE
SKED	1130	1500	1520
ETE	29	5	29
MAG BRG	329	063	155
DIST (nm)	60	6	60
OFF BLOCK	1121	1505	
TAKE OFF	1131	1508	
LAND	1205		
ON BLOCK	1208		
AIR TIME	34		
BLOCK TIME	47		
BOARDING	15(0)+1	7(5)+0	*4(2)+0
TOT ON BOARD	15(0)+1	7(5)+0	11(7)+0
DISEMBARKING	15(0)+1	0(0)+0	11(7)+0
A/C APS	8906	8906	8906
PAX	2,265	1,245	1,923
BAGGAGE	664	249 184	296
MAN AJUST	0	202 20	0
+/- FUEL	-390	390	0
FUEL @ T/O	665	735	655
T/O MASS	12,600	11,067	11,780
MAN AJUST.	0	0	0
SECTOR BURN	290	50	290
LDG MASS	12,210	11,017	11,490
OPS FUEL O/B	440	410	380
MIN FUEL REQ	1070	750	670
+/- FUEL	-390	390	0
FUEL @ DEP	680	760	670
SECTOR BURN	290	50	290
TAXI FUEL	30	30	30
FUEL @ ARR	360	670	350
TOTAL BURN	320	400	720
C of G % MAC	27	29	

Sunset/Grounding

	09 06 2024	10.06 2024
TWIL From	05 31	05 32
Sunrise	05 52	05 53
Sunset	18 17	18 18
Grounding	18 38	18 39
TWIL to	18 38	18 39

Tides

09-06-2024		10-06-2024	
Time	Tide	Time	Tide
01:56	0.6	02:35	0.6
08:04	-0.1	08:40	0.0
15:18	0.8	15:35	0.8
21:32	0.1	21:47	0.2

This aircraft is loaded in accordance with CAT.POL.MAB.100 for the [redacted]

This flight release has been prepared in accordance with MCAR Air Operat[redacted]anual

CHECK REPETITIVE ITEMS [redacted]

Captains Signature

Flight Dispatcher's Signature

5.3 Report #1 – ENB037175P (Metallurgical Evaluation of Six Samples)

Element Materials Technology
3200 S 166th Street
New Berlin, WI
53151-4141 USA

P 262 782 6344
F 262 782 3653
T 800 726 6385
info.newberlin@element.com
element.com

Dan Holland
Wipaire Inc
1700 Henry Avenue
South Saint Paul, MN 55075
dholland@wipaire.com

Date: February 20, 2025
PO Number: 155174
Quote Number: ENB0112791Q

Metallurgical Evaluation of Six Samples

Prepared by:

Mason P. Steffes, EIT
Associate Metallurgical Engineer
Mason.steffes@element.com

element

INTRODUCTION

Three samples identified as rear spreader bars which will be referred to as fittings for the purposes of this evaluation, and 3 bolts were submitted for metallurgical evaluation. This evaluation was to accompany a separate report of a failure analysis of another spreader bar.

OBJECTIVE

The objective of this investigation was to determine, if possible, whether the samples were exhibiting any signs of failure, with a particular emphasis on fatigue. The scope of this evaluation was to include visual examination, scanning electron microscopy (SEM), optical emission spectroscopy (OES), and metallographic evaluation.

CONCLUSIONS

No signs of fatigue were evident during the evaluation. However, branching cracks on the thread tips of Bolt 1 may be of interest. Determination of the cause of the cracks is beyond the scope of this evaluation. The fittings exhibited inclusions near the surface of the bolt holes which could act as sites for stress concentration.

TESTS AND RESULTS

Visual Examination

The samples are presented as received in Figures 1 through 3. The samples were examined as received for signs of failure and again after cleaning the fittings with parts cleaner and ethanol and cleaning the bolts with Alconox and ethanol. No signs of failure were evident during the visual examination.

SEM/EDS Analysis

Selected regions of the samples were examined via SEM after cleaning. SEM allows for the examination of surfaces at high magnification with great depth of field. The regions of interest were examined using secondary electrons (SE), which provide information regarding the physical morphology of the surface being examined.

SE scanning electron micrographs of the samples are presented in Figures 4 through 9. No signs of failure were evident during the SEM analysis. However, the surface condition and the coatings precluded complete examination of the surface morphology. The coating could not be removed without damaging the surface of the samples and the samples were examined as is.

Chemical Analysis

Chemical analysis of the samples was performed via OES, with the results reported in Table 1. The bolts conformed to the requirements of ASTM A29 for Grade 8640 steel when the acceptable carbon range is expanded to include product analysis tolerances per ASTM A29, Table 6. The fittings conformed to the requirements of ASTM B209 for Alloy 2024 aluminum.

element

Metallographic Evaluation

A metallographic cross-section was prepared from each sample and is presented in Figures 10 through 21. The bolt samples exhibited microstructures indicative of tempered martensite. Bolt 1 exhibited several cracks in the tips of the threads, a representative crack is measured in Figure 10. The fitting samples exhibited microstructures judged to be typical of a heat treated 2024 aluminum. The fitting samples exhibited inclusions at or near the surface of the bolt hole.

Microhardness Testing

Knoop microhardness testing was performed with a 500 gram force load on the core of the metallographic specimens. Five impressions were made and their values averaged for each sample. The results of the microhardness testing were judged to be typical for their respective alloys and condition.

This report applies only to the sample(s) tested and is not necessarily indicative of the qualities of the apparently similar or identical products. The findings presented herein are given with a reasonable degree of engineering certainty using currently available data. Element New Berlin reserves the right to supplement or amend this report should additional information become available.

If you have any questions concerning the contents of this report, please contact the author. It should be noted that it is our policy to retain components and sample remnants for 30 days from the date of this report, after which time they will be discarded. Please contact the author of this report should you wish to make alternate arrangements for disposition of the material.

element

Table 1a – Chemical Analysis Results
(Weight Percent)

Element	Bolt 1	Bolt 2	Bolt 3	ASTM A29 Grade 8640 Chemical Composition
Carbon	0.38	0.43	0.36	0.36 – 0.45[1]
Manganese	0.86	0.96	0.76	0.75 – 1.00
Phosphorous	0.011	0.009	0.010	0.035 max
Sulfur	0.014	0.010	0.002	0.040 max
Silicon	0.26	0.24	0.22	0.15 – 0.35
Nickel	0.45	0.46	0.44	0.40 – 0.70
Chromium	0.46	0.46	0.45	0.40 – 0.60
Molybdenum	0.21	0.22	0.20	0.15 – 0.25
Iron	Balance	Balance	Balance	Balance

Analysis completed via OES.
[1]Expanded to include product analysis tolerances per ASTM A29, Table 6.

Table 1b – Chemical Analysis Results
(Weight Percent)

Element	Fitting 1	Fitting 2	Fitting 3	ASTM B209 Alloy 2024 Chemical Composition
Silicon	0.10	0.10	0.10	0.50 max
Iron	0.23	0.25	0.26	0.50 max
Copper	4.3	4.4	4.3	3.8 – 4.9
Manganese	0.54	0.55	0.56	0.30 – 0.9
Magnesium	1.3	1.3	1.3	1.2 – 1.8
Chromium	0.01	0.01	0.01	0.10 max
Zinc	0.12	0.12	0.12	0.25 max
Titanium	0.02	0.02	0.02	0.15 max
Others, each	<0.05	<0.05	<0.05	0.05 max
Others, total	<0.15	<0.15	<0.15	0.15 max
Aluminum	Balance	Balance	Balance	Balance

Analysis completed via OES.

element

Table 2a – Knoop Microhardness Test Results

(HK 0.5)

Impression	Bolt 1	Bolt 2	Bolt 3
1	327.0	340.2	360.0
2	330.8	354.5	366.3
3	340.9	347.8	366.6
4	339.3	344.7	350.6
5	347.9	347.3	345.9
Average	**337**	**347**	**358**

Tested in accordance with ASTM E384.

Table 2b – Knoop Microhardness Test Results

(HK 0.5)

Impression	Fitting 1	Fitting 2	Fitting 3
1	131.2	121.1	114.9
2	133.8	118.2	123.4
3	121.6	130.5	117.6
4	135.5	127.6	128.5
5	129.5	114.7	136.6
Average	**130**	**122**	**124**

Tested in accordance with ASTM E384.

element

(a)

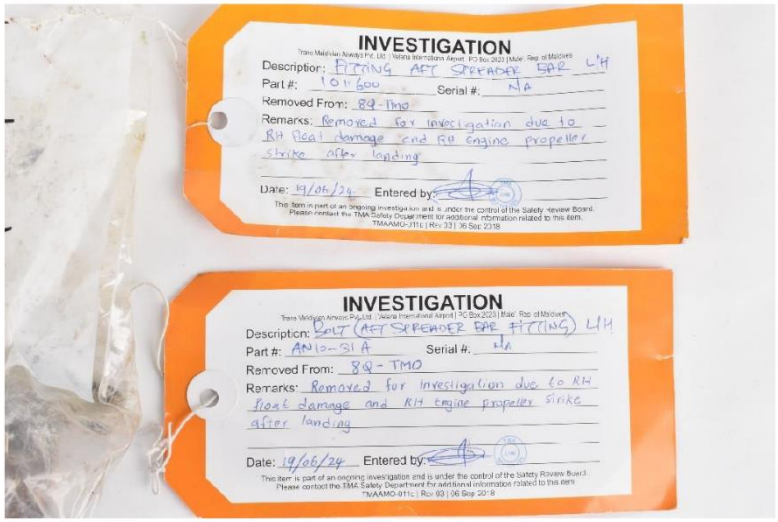

(b)

Fig. 1 **The samples designated Bolt 1 and Fitting 1 are presented as received in (a) with identifying information presented in (b). The scale is in millimeters.**

element

(a)

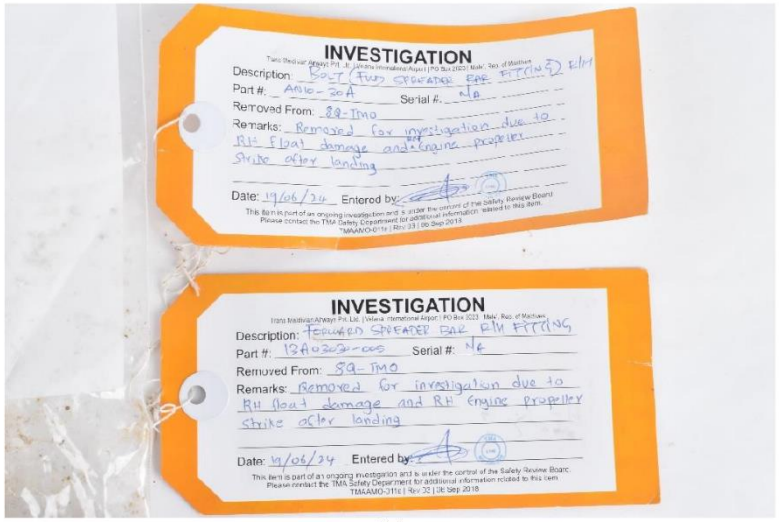

(b)

Fig. 2 **The samples designated Bolt 2 and Fitting 2 are presented as received in (a) with identifying information presented in (b). The scale is in millimeters.**

element

(a)

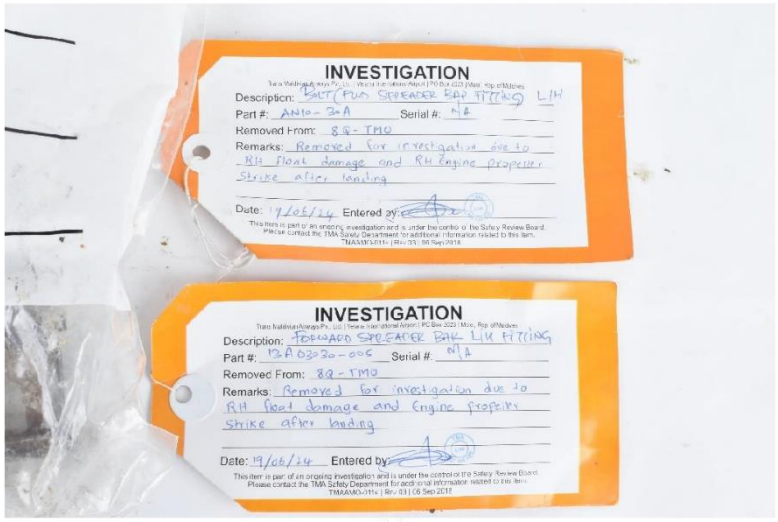

(b)

Fig. 3 **The samples designated Bolt 3 and Fitting 3 are presented as received in (a) with identifying information presented in (b). The scale is in millimeters.**

element

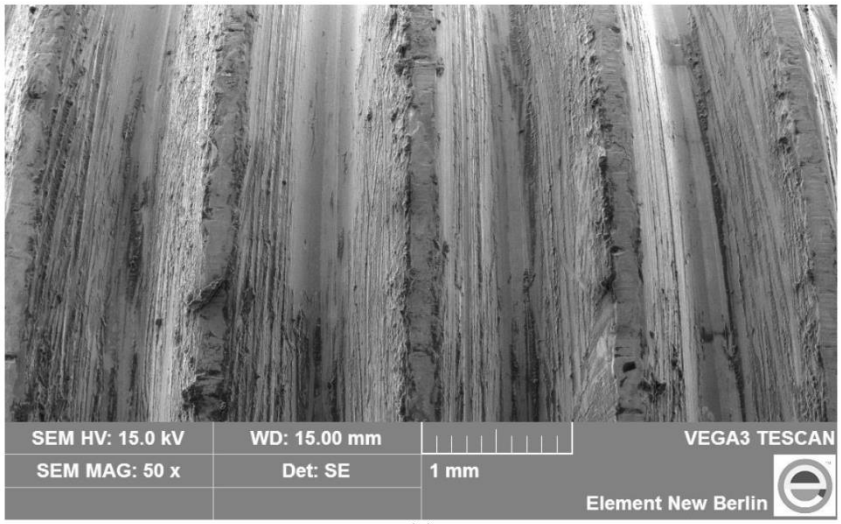

(a)

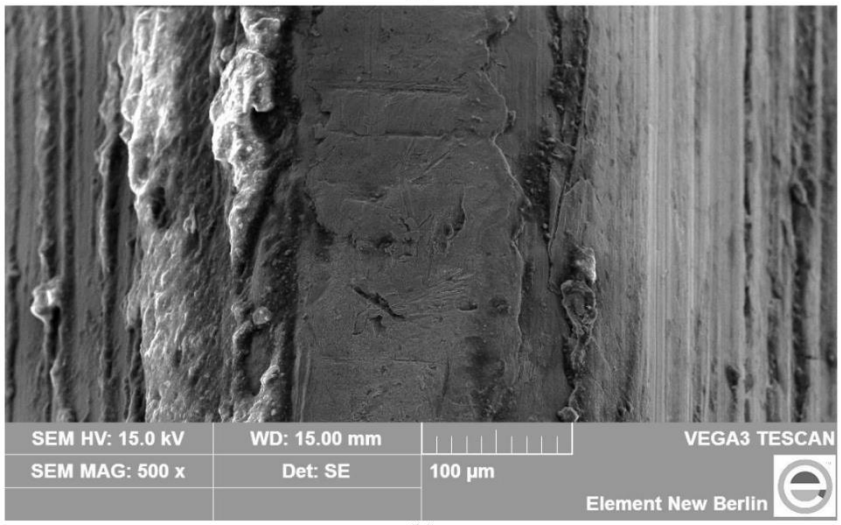

(b)

Fig. 4 **A scanning electron micrograph of a representative area of Bolt 1 is presented in (a) and at higher magnification in (b). No indications of cracking or failure were evident.**

element

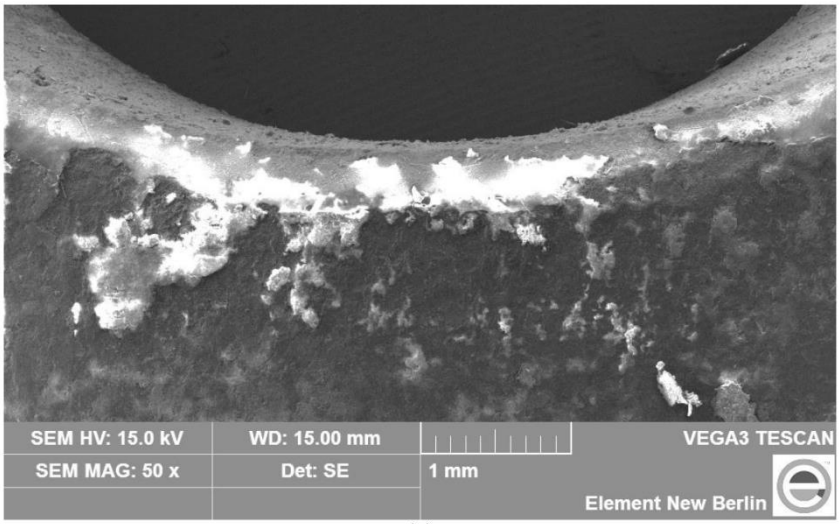

(a)

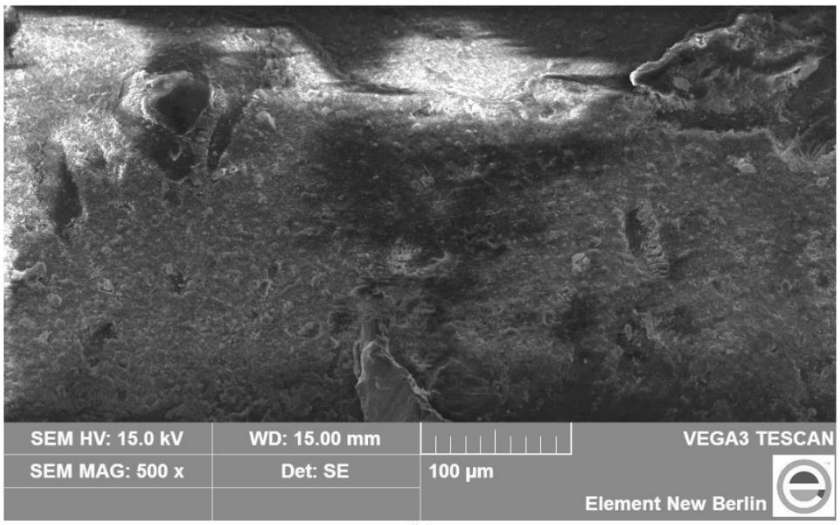

(b)

Fig. 5 **A scanning electron micrograph of a representative area of Fitting 1 is presented in (a) and at higher magnification in (b). No indications of cracking or failure were evident.**

element

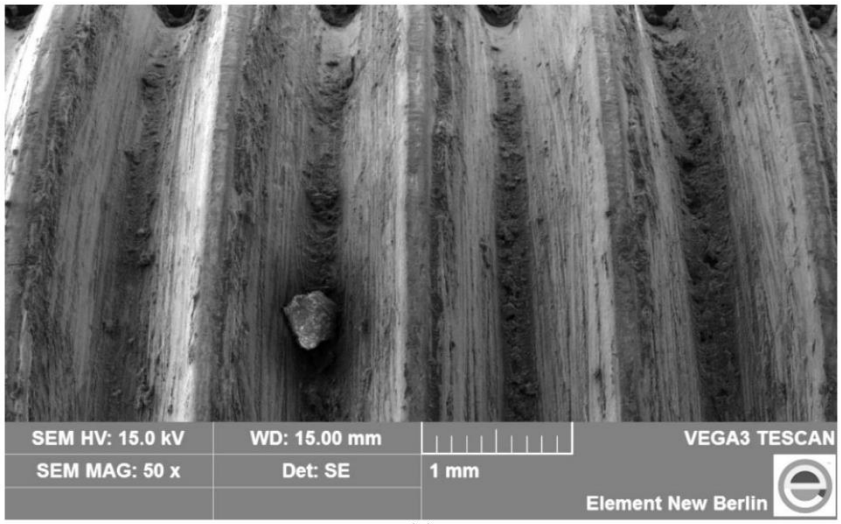

(a)

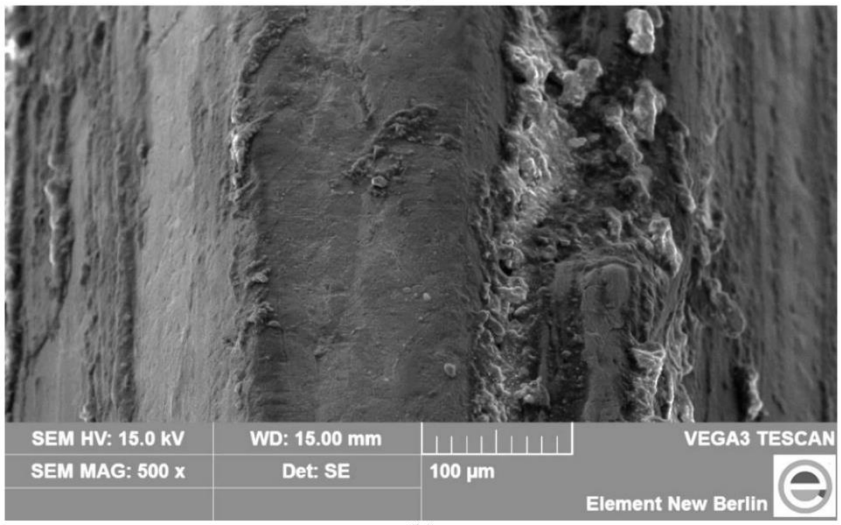

(b)

Fig. 6 **A scanning electron micrograph of a representative area of Bolt 2 is presented in (a) and at higher magnification in (b). No indications of cracking or failure were evident.**

element

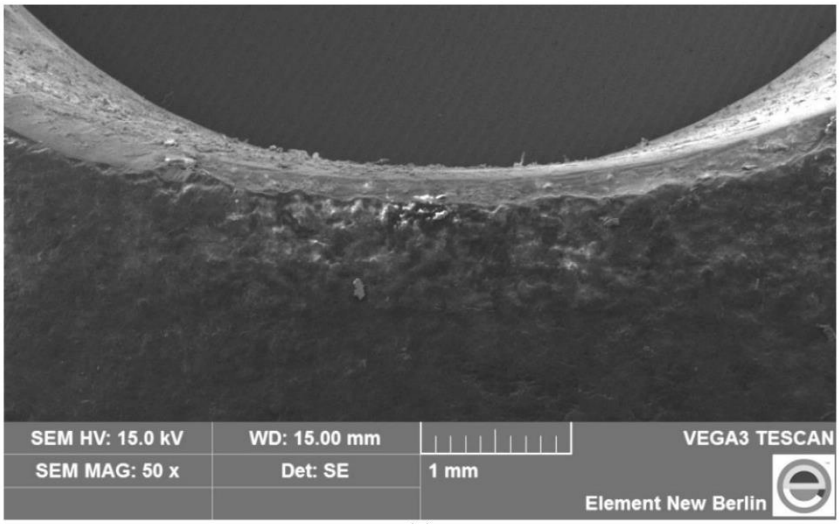

(a)

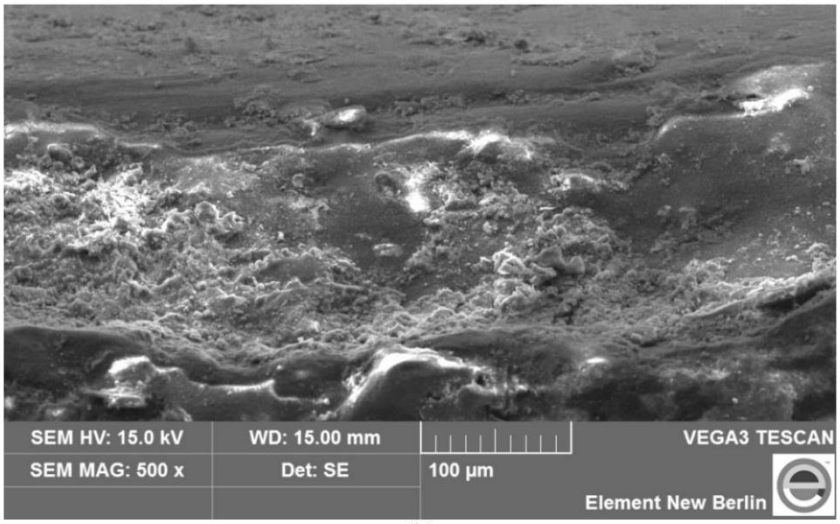

(b)

Fig. 7 **A scanning electron micrograph of a representative area of Fitting 2 is presented in (a) and at higher magnification in (b). No indications of cracking or failure were evident.**

element

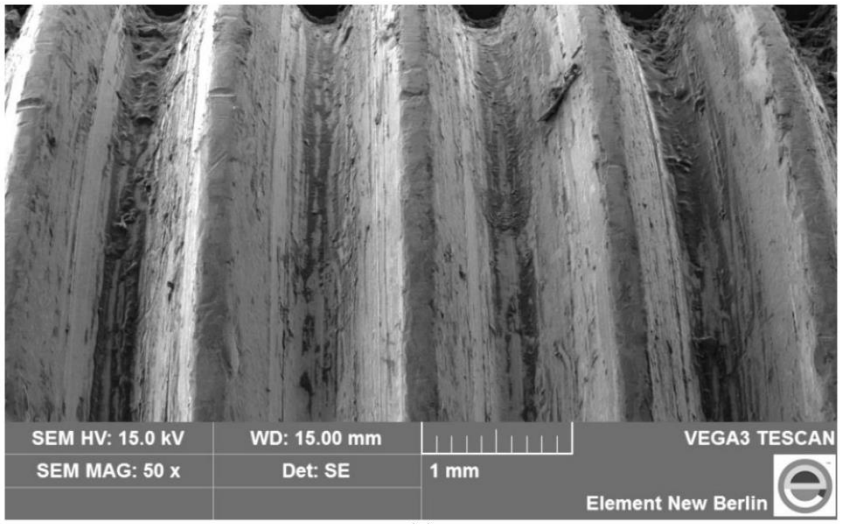

(a)

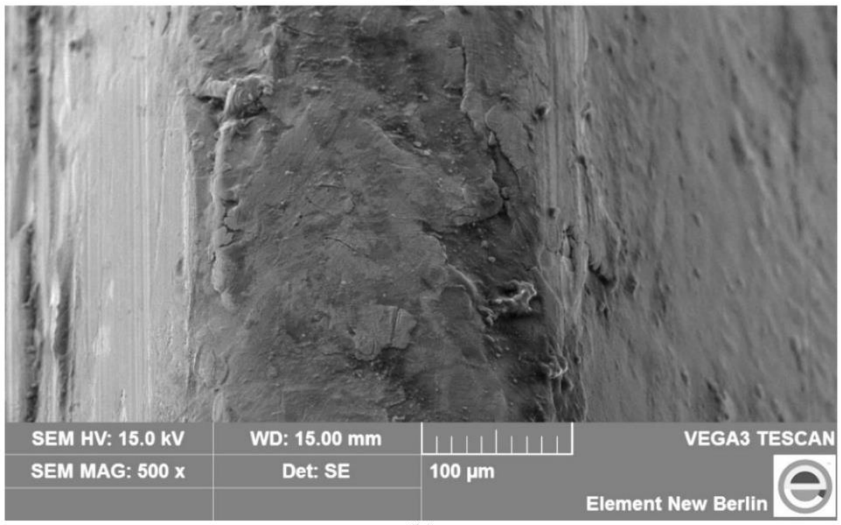

(b)

Fig. 8 **A scanning electron micrograph of a representative area of Bolt 3 is presented in (a) and at higher magnification in (b). No indications of cracking or failure were evident.**

element

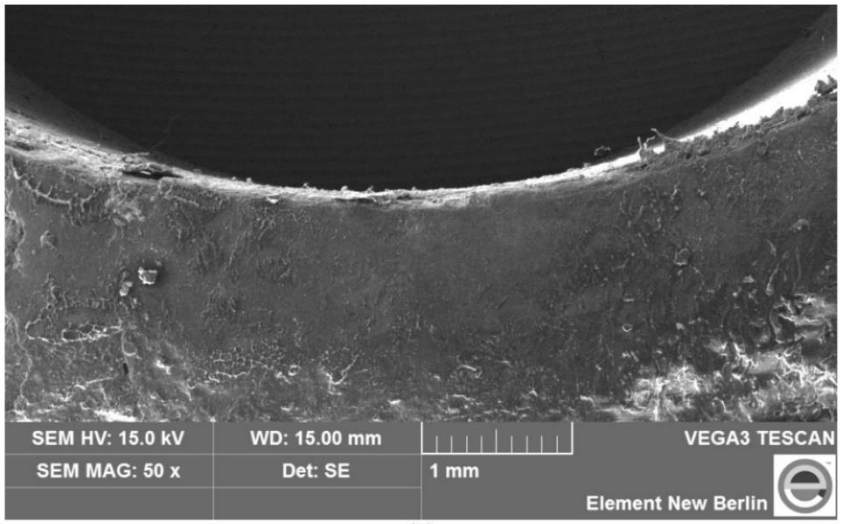

(a)

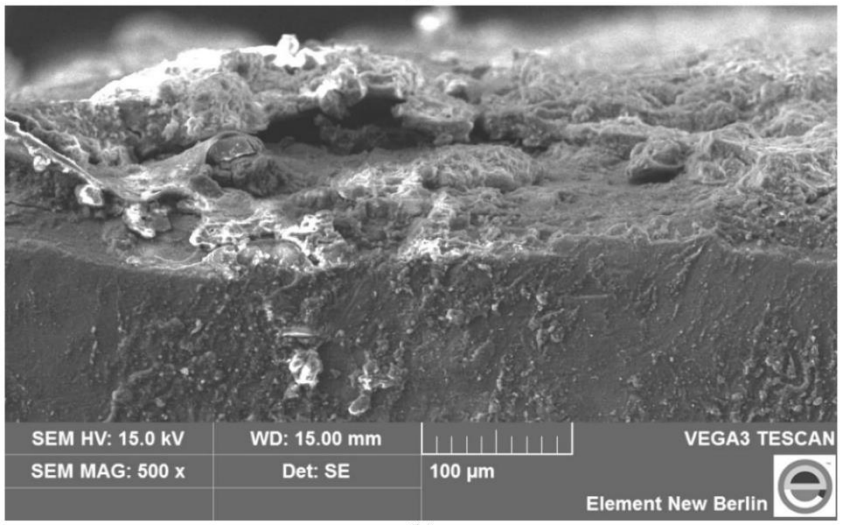

(b)

Fig. 9 **A scanning electron micrograph of a representative area of Fitting 3 is presented in (a) and at higher magnification in (b). No indications of cracking or failure were evident.**

element

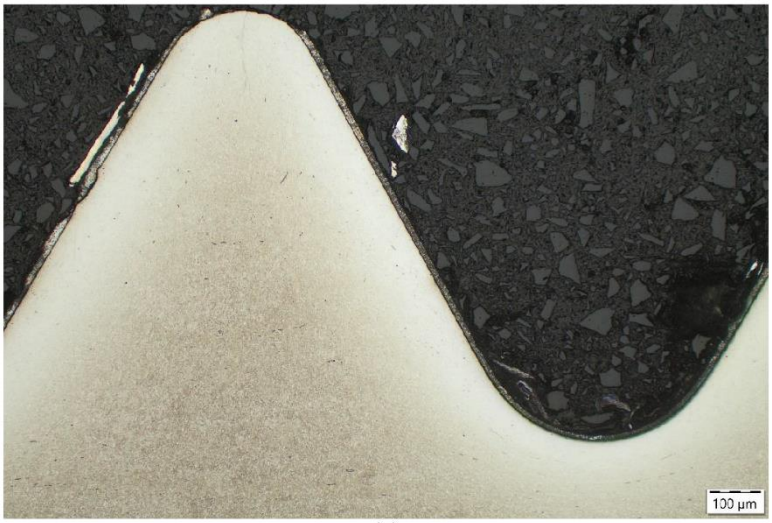

(a)

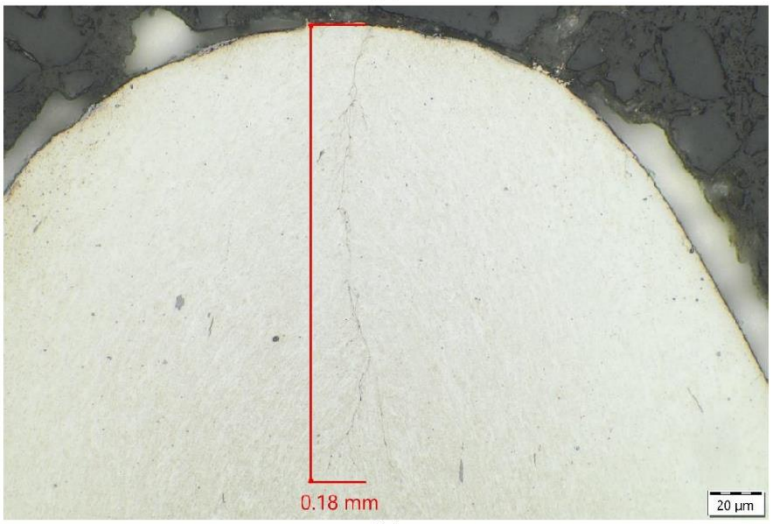

(b)

Fig. 10 **The surface of the metallographic specimen prepared from Bolt 1 is presented in (a) and a crack in the tip of the thread is presented at higher magnification in (b). The microstructure was indicative of tempered martensite. Grain flow from the forming operation is evident in the view. The crack is measured in the view. 2% Nital.**

element

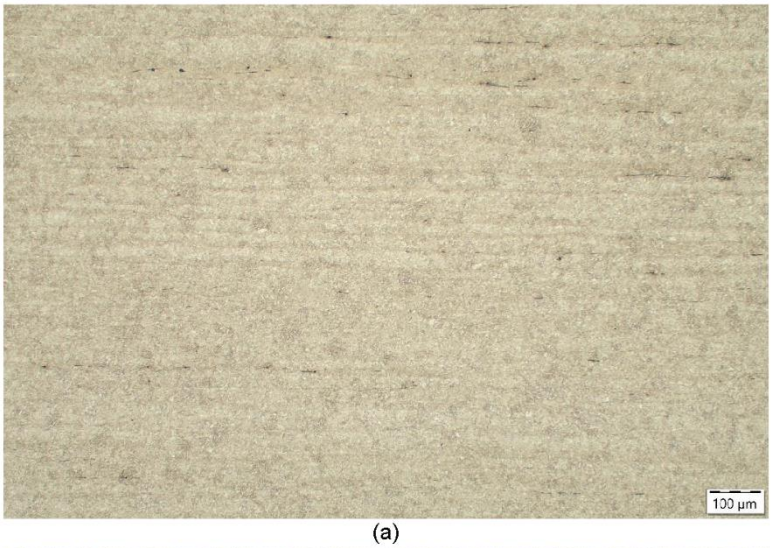

(a)

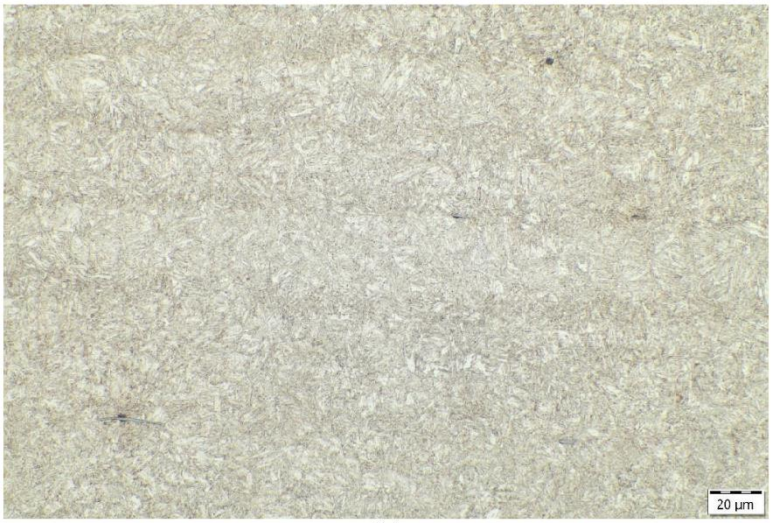

(b)

Fig. 11 **The core of the metallographic specimen prepared from Bolt 1 is presented in (a) and at a higher magnification in (b). The microstructure was indicative of tempered martensite. Sulfide inclusions are evident in the view. 2% Nital.**

element

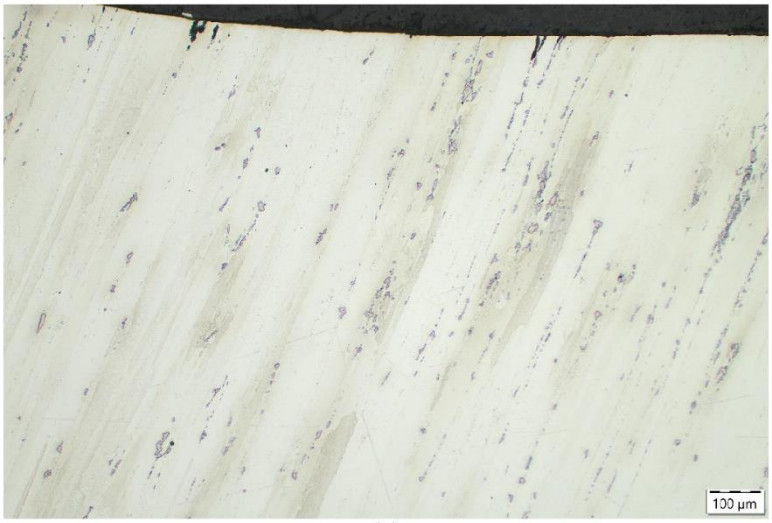

(a)

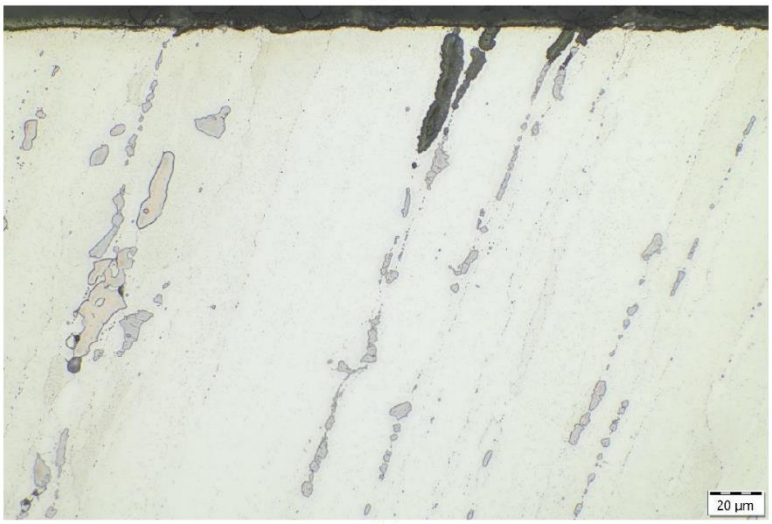

(b)

Fig. 12 **The surface of the metallographic specimen prepared from Fitting 1 is presented in (a) and at higher magnification in (b). The microstructure was typical of a 2024-T3 aluminum. Inclusions are evident near the surface. 20% NaOH.**

element

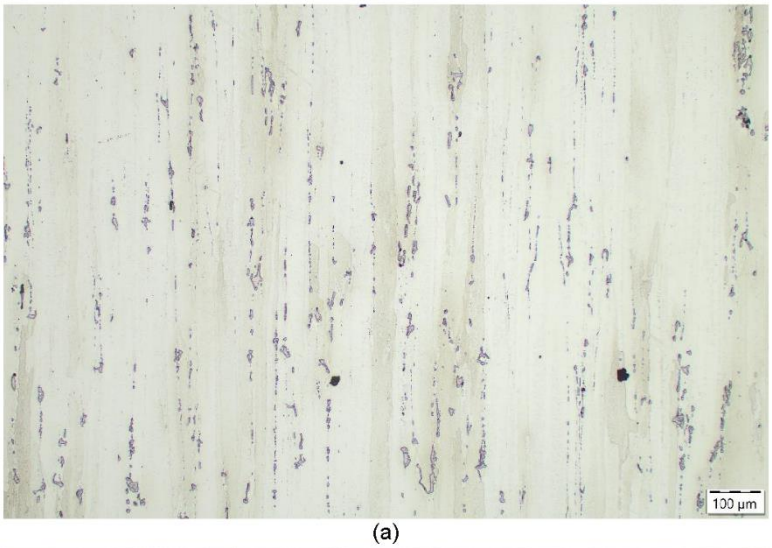

(a)

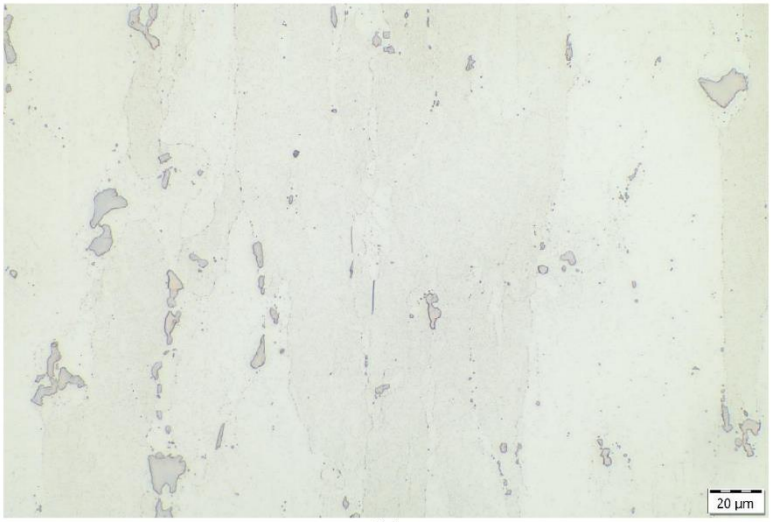

(b)

Fig. 13 **The core of the metallographic specimen prepared from Fitting 1 is presented in (a) and at higher magnification in (b). The microstructure was typical of a 2024-T3 aluminum. 20% NaOH.**

element

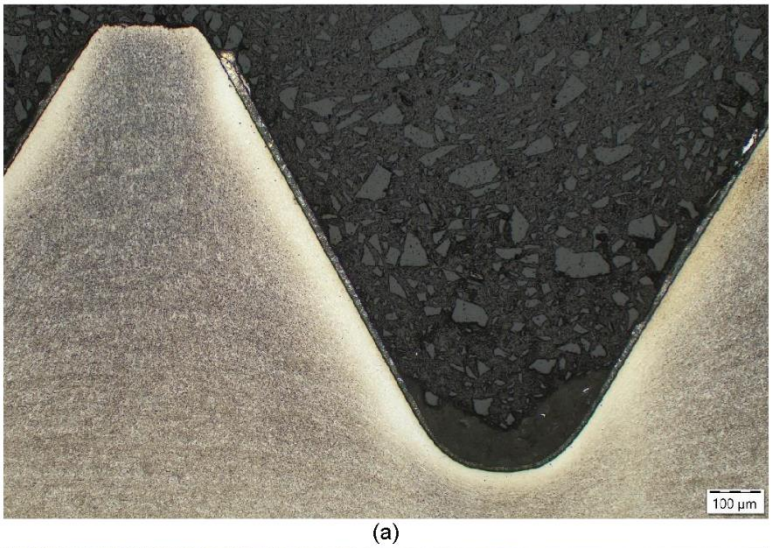

(a)

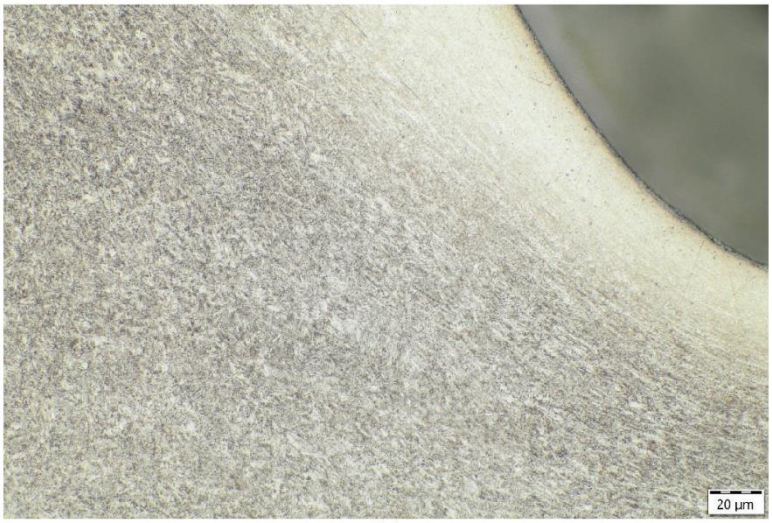

(b)

Fig. 14 **The surface of the metallographic specimen prepared from Bolt 2 is presented in (a) and the root of the thread is presented at higher magnification in (b). The microstructure was indicative of tempered martensite. Grain flow from the forming operation is evident in the view. 2% Nital.**

element

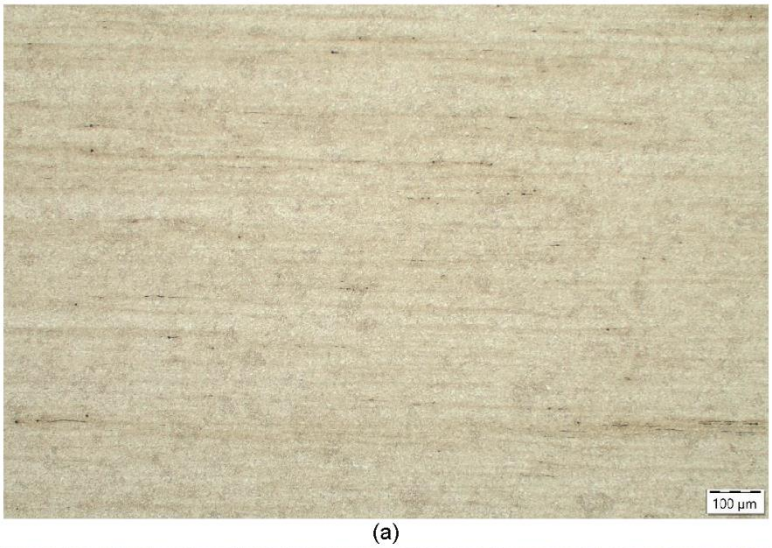

(a)

(b)

Fig. 15 **The core of the metallographic specimen prepared from Bolt 2 is presented in (a) and at higher magnification in (b). The microstructure was indicative of tempered martensite. Sulfide inclusions are evident in the view. 2% Nital.**

element

(a)

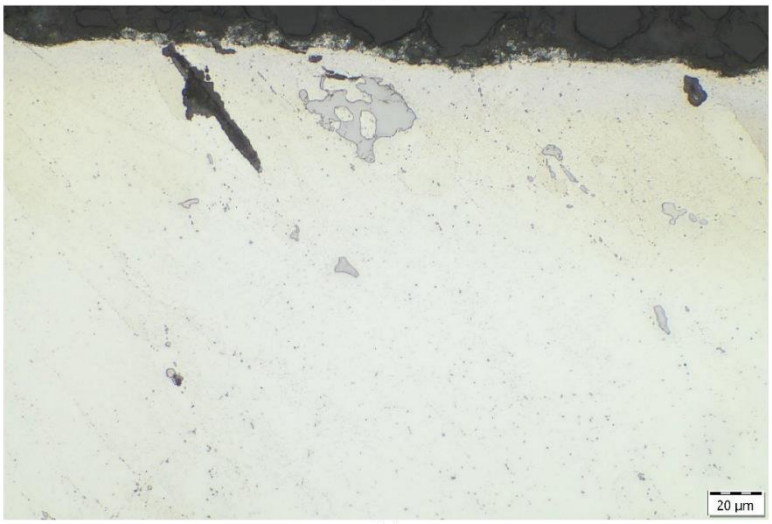

(b)

Fig. 16 **The surface of the metallographic specimen prepared from Fitting 2 is presented in (a) and at higher magnification in (b). The microstructure was typical of a 2024-T3 aluminum. Near surface inclusions are evident in the view. 20% NaOH.**

element

(a)

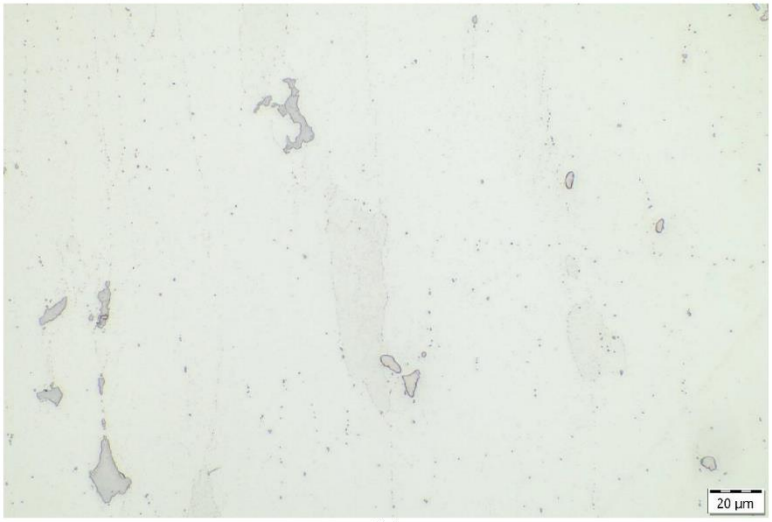

(b)

Fig. 17 **The core of the metallographic specimen prepared from Fitting 2 is presented in (a) and at higher magnification in (b). The microstructure was typical of a 2024-T3 aluminum. 20% NaOH.**

element

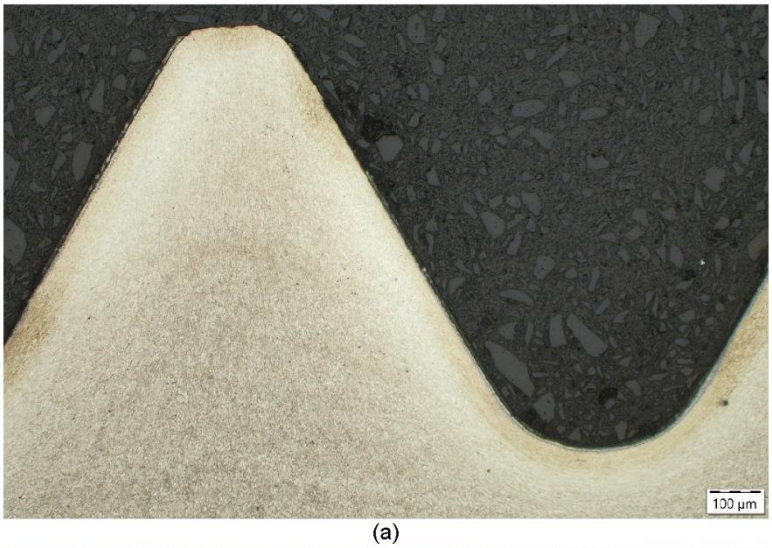

(a)

(b)

Fig. 18 **The surface of the metallographic specimen prepared from Bolt 3 is presented in (a) and the root of the thread is presented at higher magnification in (b). The microstructure was indicative of tempered martensite. Grain flow from the forming operation is evident in the view. 2% Nital.**

element

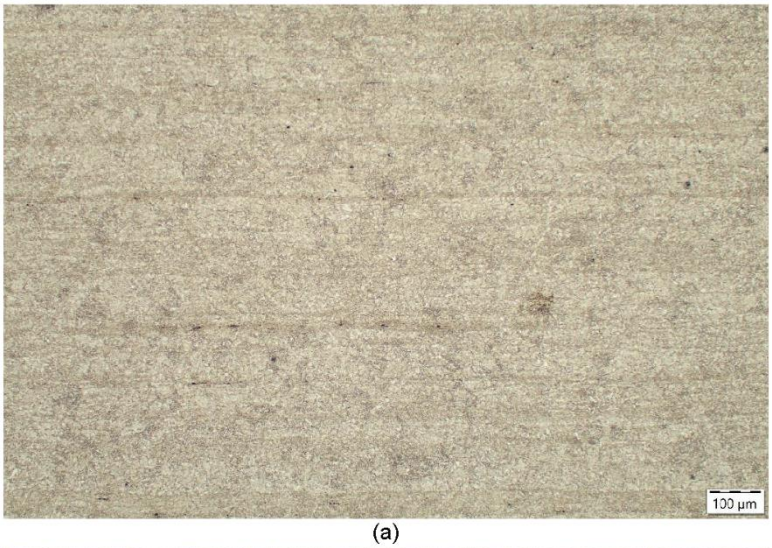

(a)

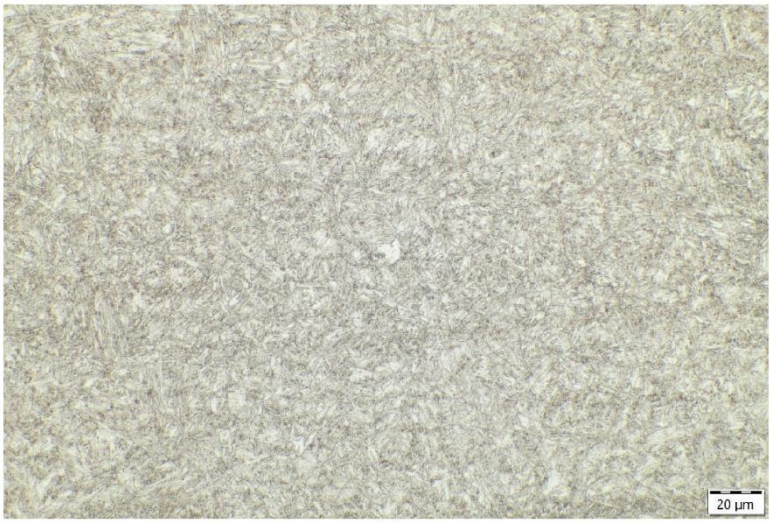

(b)

Fig. 19 **The core of the metallographic specimen prepared from Bolt 3 is presented in (a) and at higher magnification in (b). The microstructure was indicative of tempered martensite. Sulfide inclusions are evident in the view. 2% Nital.**

element

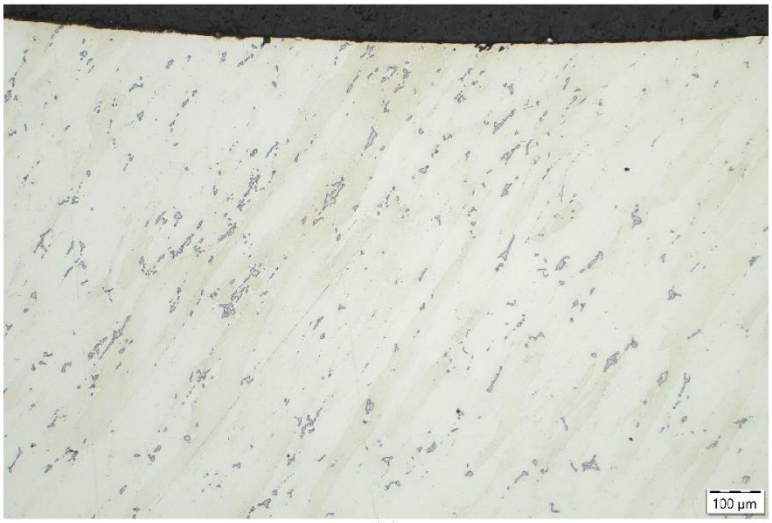

(a)

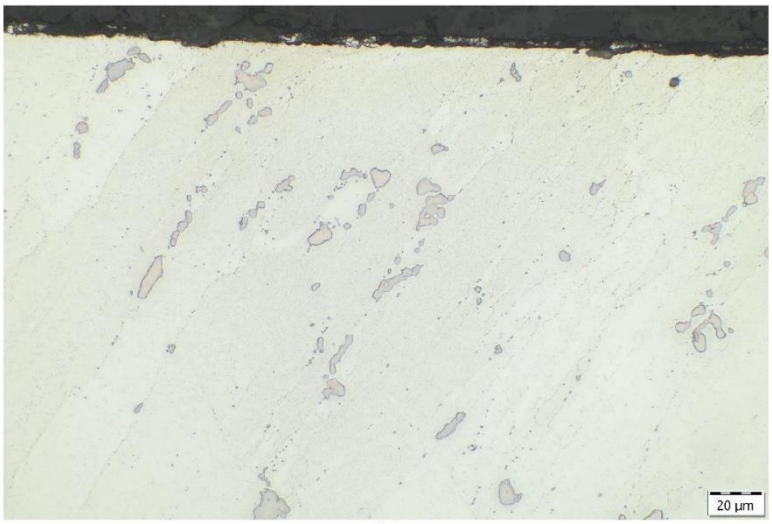

(b)

Fig. 20 **The surface of the metallographic specimen prepared from Fitting 3 is presented in (a) and at higher magnification in (b). The microstructure was typical of a 2024-T3 aluminum. 20% NaOH.**

element

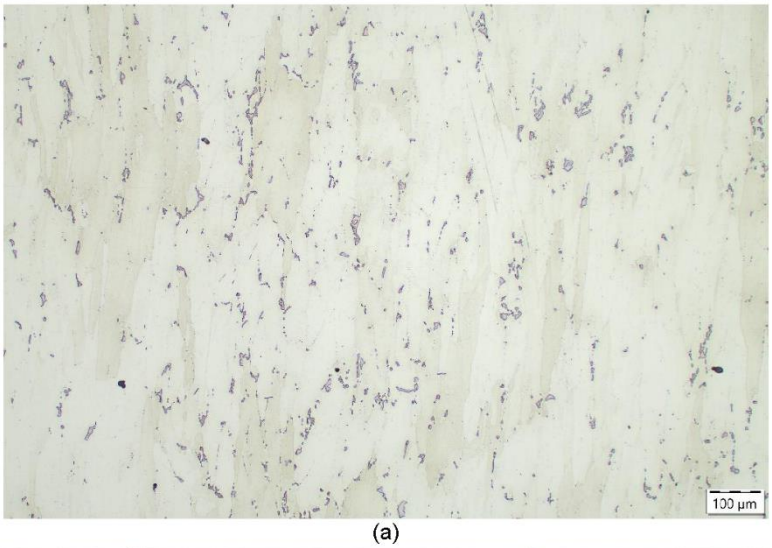

(a)

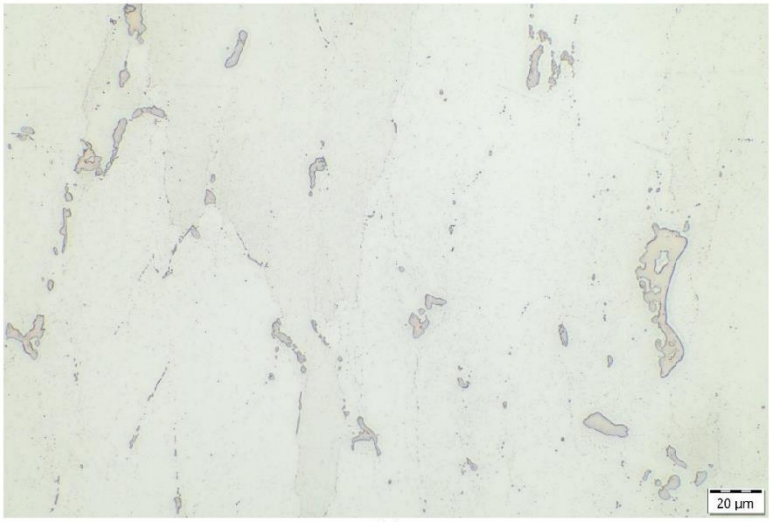

(b)

Fig. 21 **The core of the metallographic specimen prepared from Fitting 3 is presented in (a) and at higher magnification in (b). The microstructure was typical of a 2024-T3 aluminum. 20% NaOH.**

5.4 Report #2 - ENB037181P (Metallurgical Evaluation of Cracked Fittings)

element

Element Materials Technology
3200 S 166th Street
New Berlin, WI
53151-4141 USA

P 262 782 6344
F 262 782 3653
T 800 726 6385
info.newberlin@element.com
element.com

Mr. Dan Holland
Wipaire Inc
1700 Henry Avenue
South Saint Paul, MN, 55075
dholland@wipaire.com

Date:	March 12, 2025
Report Number:	ENB037181P
Client Reference:	P.O. No. 155174
Element Quote No.	ENB0112084Q

Metallurgical Evaluation of Cracked Fittings

PREPARED BY:

Abbas Mohammadi, Ph.D.
Principal Metallurgical Engineer
abbas.mohammadi@element.com

element

INTRODUCTION

A fractured fitting, P/N 13A03030-004, was received from Wipaire Inc. for evaluation as the component had failed in service. The fitting featured twin parallel lugs and was reported to be manufactured from Aluminum 2024-T3. Its surface finish consisted of three layers, chromate conversion, epoxy primer and white paint. It was stated that the fitting was part of the aircraft located in an area far from high heat sources. The aircraft operated exclusively in a tropical environment and spent more time docked in the sea water than indoors. No precise details concerning the service life were provided.

OBJECTIVE

The objective of this investigation was to identify the cause for the failure of the fittings if possible. The scope of this evaluation was to include visual inspection, scanning electron microscopy (SEM), energy dispersive X-ray spectroscopy (EDS), chemical analysis, hardness testing, and metallography.

CONCLUSIONS

The conclusion of this investigation is that the fitting failed due to intergranular stress corrosion cracking (IGSCC), where intergranular cracking occurred in areas subjected to applied stress while exposed to a corrosive environment such as seawater.

The crack initiated at a pitting corrosion site that developed at the bore of lug. The pitting corrosion likely formed as a result of crevice corrosion between the bore and the bolt. The presence of inadequate lubrication may have failed to protect the surface. Additionally, if a dissimilar material bolt was used, galvanic corrosion could have been a contributing factor. The primary crack propagated through the lug to the tip of the fitting in a direction consistent with the applied loads. The cracking on both fitting lugs were judged to be similar.

Microscopic examination of the fracture surface and the area adjacent to the crack origin revealed intergranular cracking along elongated grain boundaries. The failure of the fitting was determined to be related to applied stresses and the corrosive environment, with no evidence of overload or fatigue fracture observed at the crack origin or along the fracture surface.

Visual and SEM/EDS analysis of the sample showed evidence of severe surface corrosion, pitting, and intergranular corrosion. EDS analysis of the corrosion products identified elements consistent with corrosion, with chlorine detected at a sufficient concentration to contribute to the process. Secondary intergranular cracks were evident on the surface adjacent to the crack origin. Additionally, microscopy examination revealed the distribution of coarse intermetallic particles, and EDS analysis indicated that these intermetallic particles consist of a copper-rich element. These areas were particularly susceptible to corrosion attack.

The main body of the part was found to be epoxy-primed and painted. However, the paint and epoxy primer layers were absent in the areas where cracks originated, likely due to surface wear during in-service operation. The exposure of these areas most likely contributed to the initiation of stress corrosion cracking.

The measured hardness and chemical composition analysis confirmed that the material was consistent with Aluminum 2024-T3.

element

TESTS AND RESULTS

Visual Examination

The overall view of the as-received failed fitting, designated as Part A is shown in Figure 1, with a close-up examination presented in Figure 2. Part A had twin parallel lugs, identified as Lug 1 and Lug 2 in Figure 1. Lug 1 was fractured at its bore, and the broken mating piece was not submitted for evaluation. Lug 2 exhibited a through-crack extending from the bore to the edge of the lug, at a similar location as Lug 1 had fractured. For further investigation, Lug 1 was selected and sectioned into two parts, designated as Sections A and B as shown in Figure 3.

The visual appearance of Part A exhibits features indicative of an epoxy-primed and painted surface. However, on the majority of both lug surfaces, including the bores and crack sites, the epoxy primer and paint layers were not evident, as shown in Figures 2 through 5. Rust-colored corrosion products and severe corrosion pitting were observed in the bores and along the primary cracks.

Figure 5 shows an overview image of the fracture surface of Section A exhibiting rust-colored deposits, particularly at the assumed crack origin at the bore of the component. A higher-magnification image of the fracture surface revealed intergranular cracking features at the crack origin, as shown in Figure 6. It should be noted that significant mechanical damage was present on the fracture surface, limiting the observation of crack propagation features.

SEM and EDS Analysis

The fracture edge on the backside of Section A was examined using SEM, as shown in Figures 7 and 8. SEM examination revealed the presence of intergranular cracks along elongated grain boundaries, with corrosion products observed on the fracture surface and adjacent to the crack origin.

The SEM examination of the surface of Section B is shown in Figures 9 to 11. The surface adjacent to the crack origin exhibited extensive corrosion products, particularly along the secondary cracks. The specimen was also analyzed using EDS to determine the composition of the corrosion products. EDS analysis was conducted at the two locations indicated in Figure 11, and the results are presented in Table 1a. The analysis revealed high carbon, oxygen, and chlorine contents. The significant presence of chlorine, likely in the form of chlorides, indicates a corrosive environment for a Type 2024-T3 aluminum alloy.

Fractography of the crack origin on Section A is shown in Figures 12 and 13. The fracture surface displayed intergranular cracking features at the crack origin. However, severe post fracture mechanical damage obscured any features related to the crack propagation path.

Chemical Analysis Results

The chemical composition of Part A was determined using inductively coupled plasma optical emission spectroscopy (ICP-OES) and the results are presented in Table 2. The composition was consistent with the specified Type 2024 aluminum alloy. There were no anomalies or deficiencies present in the composition that could account for the corrosion of the fittings.

Birnell Hardness Results

Brinell hardness testing was conducted on the backside surface of Section A and the test results are presented in Table 3. The sample exhibited a hardness consistent with a Type 2024 aluminum in the T3 condition.

Metallography
An optical microscopy image of the surface on the backside of Section A, adjacent to the crack origin and corresponding to Figure 8, is shown in Figures 14 and 15. The surface was polished to a mirror finish and then etched using Keller's reagent. The microstructure exhibited significant secondary intergranular cracks along elongated grain boundaries. A high-magnification image of the secondary cracks revealed the distribution of precipitates within the matrix and along the grain boundaries, as shown in Figure 15. Extensive corrosion attacks were observed in these precipitate-rich areas.

To further investigate the cracking mechanism, the surface studied in Figure 14 was polished to a mirror finish using oxide polishing suspensions (OPS). Backscatter electron (BSE) images of the polished surface are shown in Figures 16 and 17. Similar to the optical microscopy observations, numerous secondary cracks were observed originating from the primary crack. Additionally, precipitates were evident within the base metal. EDS analysis of these precipitates, shown in Figure 17 and summarized in Table 1b, revealed two types of precipitates, Al-Cu-Fe-Mn and Al-Cu (Copper-rich) containing particles. EDS analysis of the corrosion products along these particles exhibited high concentration of Sulfur that could be associated with the corrosion at this region.

element

Table 1a - EDS Results, Crack Origin
(Relative Weight Percent)

Element	Location 1	Location 2
Aluminum	27.9	13.0
Copper	---	0.7
Magnesium	0.6	---
Sodium	0.3	---
Nitrogen	0.9	---
Silicon	0.2	
Calcium	0.6	0.8
Sulfur	0.8	0.9
Chlorine	12.9	15.2
Carbon	6.1	37.5
Oxygen	49.7	32.0

--- = Not Detected
Analysis completed using Energy Dispersive X-ray Spectroscopy (MA-15).
EDS analysis can detect and quantify elements from atomic no. 5 (boron) and greater on the Periodic Table. Relative percentages of the detected elements can be determined and are normalized to total 100%. Therefore, the results of these analyses are relative rather than absolute values.
Blue color indicates primary elements in base alloys.
Red color indicates elements that promote corrosion and stress corrosion cracking.
Brown color indicates oxide rich deposits such as corrosion products.

Table 1b - EDS Results, Alloy constituents
(Relative Weight Percent)

Element	Location 1	Location 2	Location 3 (Corrosion Products)
Aluminum	55.0	10.1	31.8
Copper	6.8	74.5	2.8
Manganese	7.4	---	---
Magnesium	0.7	2.8	0.6
Silicon	4.6	---	---
Iron	12.0	1.1	---
Calcium	---	0.8	0.5
Carbon	10.9	5.3	8.7
Oxygen	2.7	4.9	53.0
Sulfur	---	0.5	2.6

--- = Not Detected
Analysis completed using Energy Dispersive X-ray Spectroscopy (MA-15).
EDS analysis can detect and quantify elements from atomic no. 5 (boron) and greater on the Periodic Table. Relative percentages of the detected elements can be determined and are normalized to total 100%. Therefore, the results of these analyses are relative rather than absolute values.

element

Table 2 - Chemical Analysis Results
(Weight Percent)

Element	P/N 13A03030-004	Requirements[1]
Carbon	<0.01	NA
Sulfur	<0.01	NA
Copper	4.0	3.8-4.9
Manganese	0.5	0.30-0.9
Magnesium	1.4	1.2-1.8
Silicon	0.04	0.50 max.
Iron	0.16	0.50 max.
Zinc	0.01	0.25 max.
Chromium	<0.01	0.10 max.
Others, each	<0.05	0.05 max.
Others, Total	<0.15	0.15 max.
Aluminum	Remainder	Remainder

Analysis completed via ICP-OES (CS-03).
Carbon and sulfur contents determined via a combustion I/R technique (CA-06).
NA = Specification not specified
[1] Requirements per ASTM B210/B210M

Table 3 - Brinell Hardness Results
(HBW 10/500)

Sample	Backside - Part A
Location	Surface
Diameter 1 Reading (mm)	2.30
Diameter 2 Reading (mm)	2.27
Average Diameter (mm)	2.29
Brinell Value (HBW 10/500)	120

element

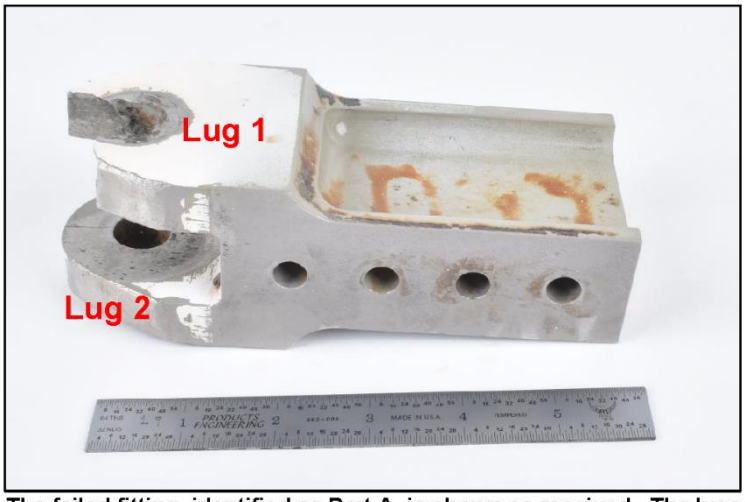

Fig. 1 The failed fitting, identified as Part A, is shown as received. The lugs are identified as Lug 1 and 2 in view. The scale is in inches.

element

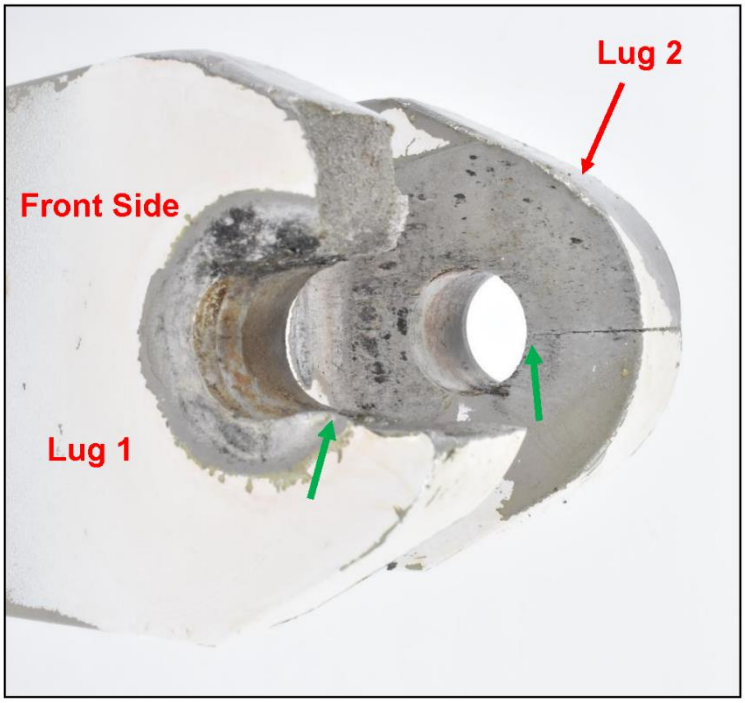

Fig. 2 A close examination of Part A is shown. The majority of the surfaces on Lug 1, Lug 2, and the bores no longer appear to have paint or epoxy layers. Rust color deposits are visible throughout the bores. Green arrows indicate crack initiation sites on at the bore of each lug.

element

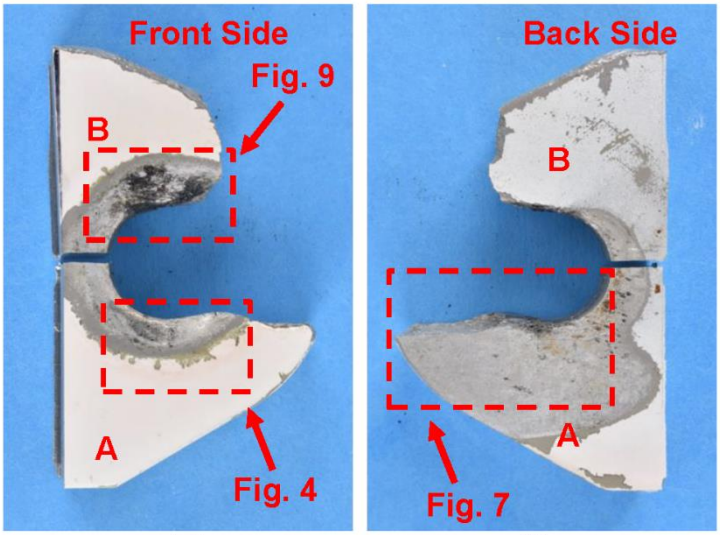

Fig. 3 A macro photograph of Lug 1 after cutting into Sections A and B for further examination is shown in (a), and after reorientation in (b). The highlighted areas are indicated for higher magnification studies, and are shown in Figure 4, 7 and 9.

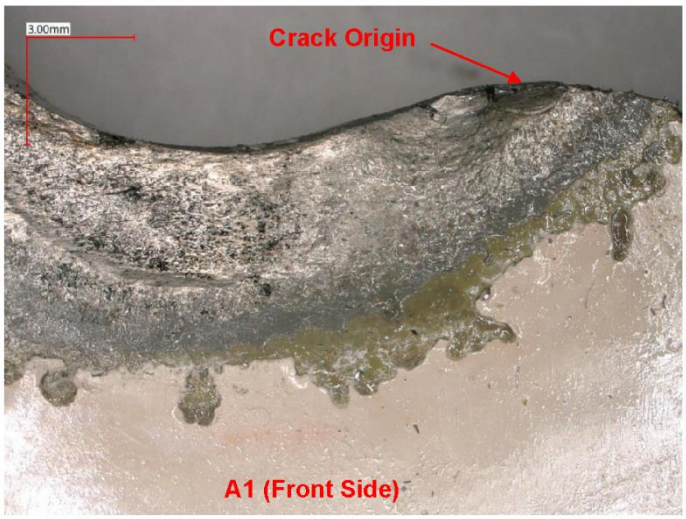

Fig. 4 An overall view of the front side of Section A, highlighted in Figure 3, exhibits features indicating that the surface where the crack initiated no longer has paint or epoxy layers. Extensive rust-colored deposits and corrosion pits are evident on the surface.

element

Fig. 5 An overall view of the surface of the crack from Section A is presented. Rust-colored deposits are evident on the surface of the bore. The fracture is on the right side of the section shown. The highlighted area is indicated for a higher magnification study, as shown in Figure 6.

Fig. 6 A higher magnification image of the fracture surface reveals corrosion deposits and intergranular cracking corresponding to the highlighted area from Figure 5.

element

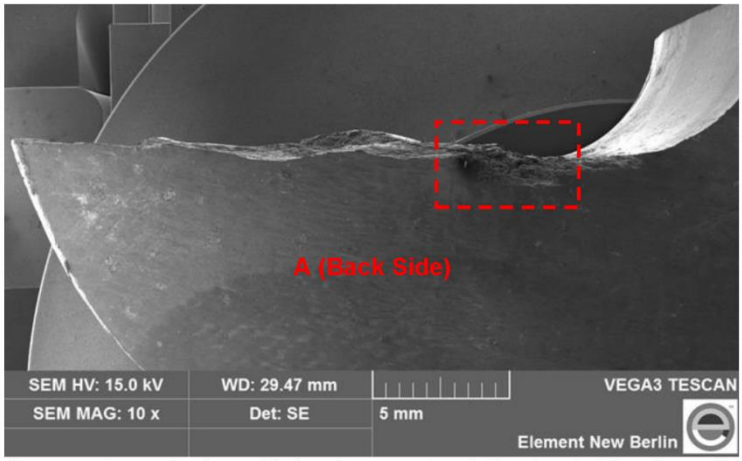

Fig. 7 A secondary electron (SE) micrograph of the backside view of Section A as indicated in Figure 3 shows the crack origin site and the fracture extending from the bore to the end of the fitting. The highlighted area is likely the crack initiation site and is shown at a higher-magnification in Figure 8.

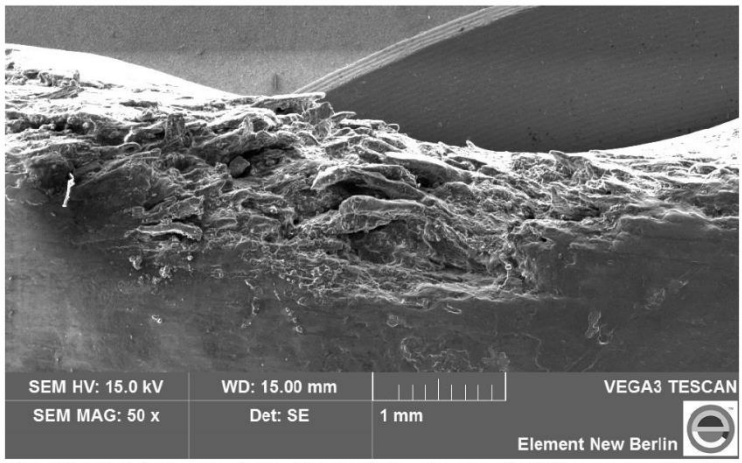

Fig. 8 The highlighted area from Figure 7 is shown at higher magnification. The surface reveals the crack origin region with surface pitting and intergranular cracking features.

element

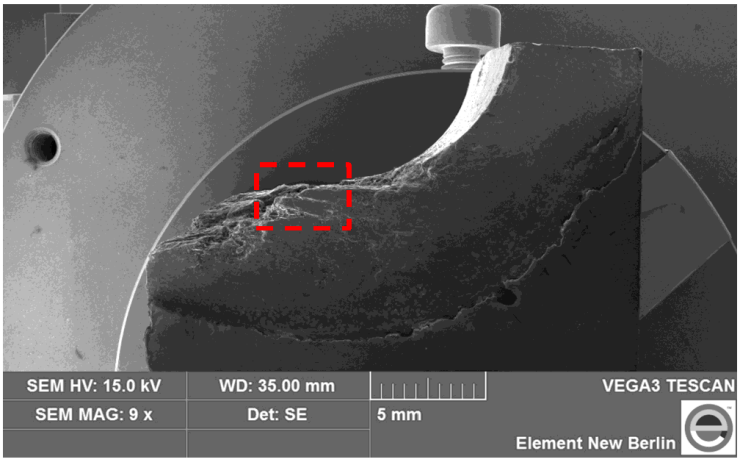

Fig. 9 An SE image of the front side of Section B is presented, including the crack origin site and propagation path. The position of this surface is defined in Figure 3. The highlighted area is selected for higher magnification SEM analysis, presented in Figure 10.

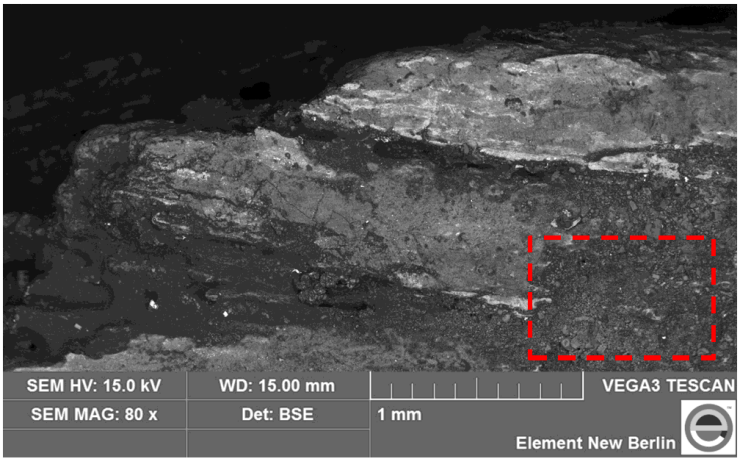

Fig. 10 A backscattered electron (BSE) micrograph shows the area indicated in Figure 10 at a higher magnification. The surface exhibits a significant amount of corrosion products. The highlighted area is further examined in Figure 11 using SEM/EDS analysis

element

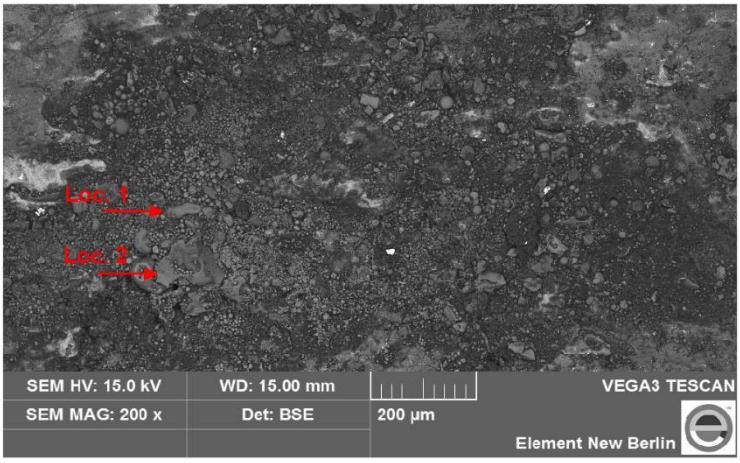

Fig. 11 The highlighted area from Figure 10 is shown at higher magnification. The surface exhibits accumulated corrosion products. EDS analysis was conducted at two locations, as indicated by the arrows and labels in view. The results are presented in Table 1.

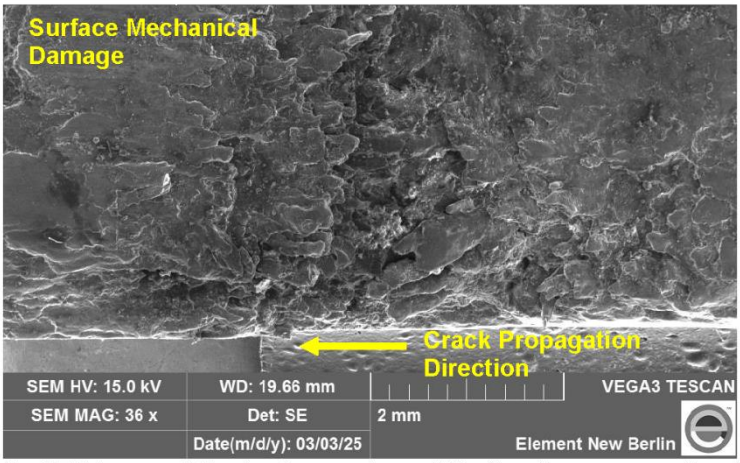

Fig. 12 An SEM image of the fracture surface of Section A, corresponding to Figure 7, is presented. The fracture surface exhibits intergranular cracking at the crack origin, which is at the center of the image, followed by post fracture mechanical damage along the crack propagation path, located on the left side of the image.

element

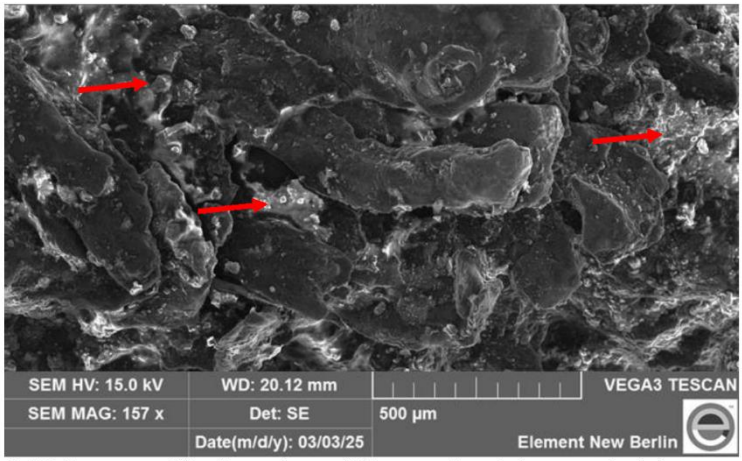

Fig. 13 A higher magnification view of the crack origin reveals intergranular cracking. Corrosion deposits are evident on the fracture surface and along the grain boundaries as indicated by red arrows.

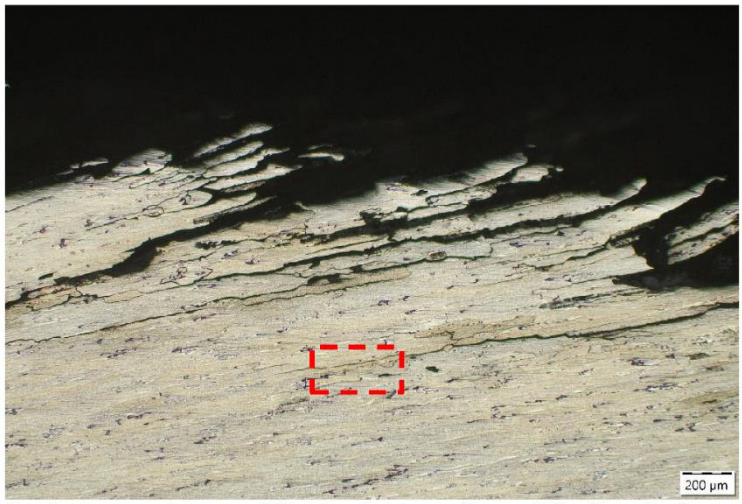

Fig. 14 A microscopy image of the backside surface of Section A, through the region indicated in Figure 8, is presented, showing secondary intergranular cracks adjacent to the primary crack. The secondary cracks propagated along elongated grain boundaries. The highlighted area was selected for a higher-magnification study, presented in Figure 15. Keller's reagent.

element

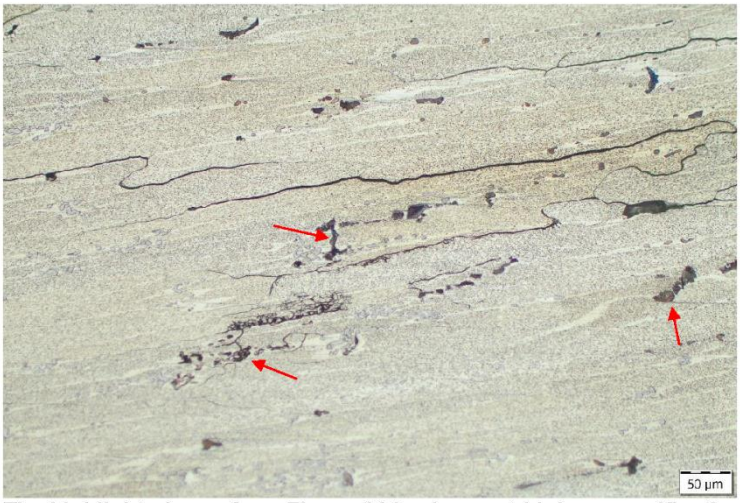

Fig. 15 The highlighted area from Figure 14 is shown at higher magnification. The surface exhibits intergranular cracks and the formation of precipitates along grain boundaries. Corrosion attack is evident around the precipitates, as indicated by the red arrows. Keller's reagent.

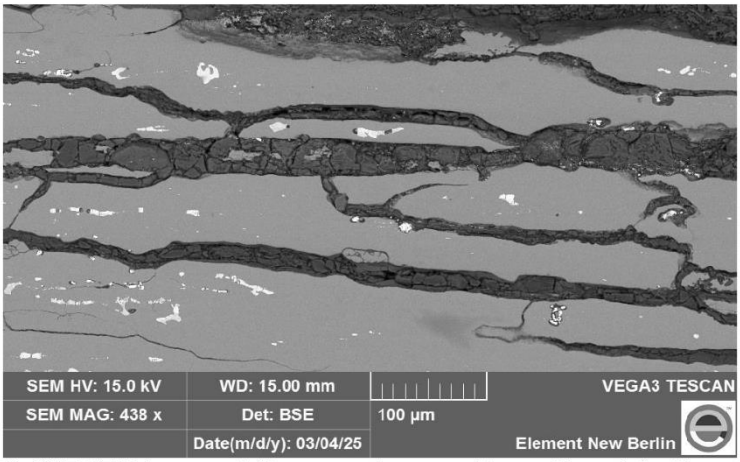

Fig. 16 A BSE-SEM image of the secondary cracking adjacent to the crack origin is presented. The white regions indicate the presence of precipitates in the aluminum alloy. As-polished.

element

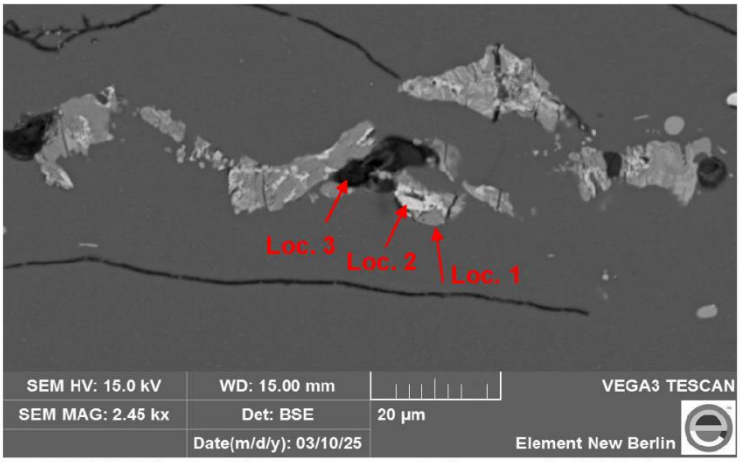

Fig. 17 **The BSE-SEM image of secondary cracks is presented at higher magnification. The surface exhibits lighter regions presenting the distribution of coarse intermetallic particles. EDS analysis of the precipitates was conducted at two locations of precipitates and at corrosion products along the precipitates, indicated by arrows and labeled in the image. The results are presented in Table 1b. As-polished.**